ARMY RESEARCH LABORATORY

Further Development of a Model for Rod Ricochet

by Steven B. Segletes

ARL-RP-164 **February 2007**

A reprint from the *International Journal of Impact Engineering*, vol. 34, pp. 899–925, 2007.

NOTICES

Disclaimers

The findings in this report are not to be construed as an official Department of the Army position unless so designated by other authorized documents.

Citation of manufacturer's or trade names does not constitute an official endorsement or approval of the use thereof.

Destroy this report when it is no longer needed. Do not return it to the originator.

Army Research Laboratory
Aberdeen Proving Ground, MD 21005-5069

ARL-RP-164 **February 2007**

Further Development of a Model for Rod Ricochet

Steven B. Segletes
Weapons and Materials Research Directorate, ARL

A reprint from the *International Journal of Impact Engineering*, vol. 34, pp. 899–925, 2007.

REPORT DOCUMENTATION PAGE

Form Approved
OMB No. 0704-0188

1. REPORT DATE *(DD-MM-YYYY)*	2. REPORT TYPE	3. DATES COVERED (From - To)
February 2007	Reprint	September 2004–March 2005

4. TITLE AND SUBTITLE
Further Development of a Model for Rod Ricochet

5a. CONTRACT NUMBER

5b. GRANT NUMBER

5c. PROGRAM ELEMENT NUMBER

6. AUTHOR(S)
Steven B. Segletes

5d. PROJECT NUMBER
AH80

5e. TASK NUMBER

5f. WORK UNIT NUMBER

7. PERFORMING ORGANIZATION NAME(S) AND ADDRESS(ES)
U.S. Army Research Laboratory
ATTN: AMSRD-ARL-WM-TD
Aberdeen Proving Ground, MD 21005-5069

8. PERFORMING ORGANIZATION REPORT NUMBER
ARL-RP-164

9. SPONSORING/MONITORING AGENCY NAME(S) AND ADDRESS(ES)

10. SPONSOR/MONITOR'S ACRONYM(S)

11. SPONSOR/MONITOR'S REPORT NUMBER(S)

12. DISTRIBUTION/AVAILABILITY STATEMENT
Approved for public release; distribution is unlimited.

13. SUPPLEMENTARY NOTES
A reprint from the *International Journal of Impact Engineering*, vol. 34, pp. 899–925, 2007.

14. ABSTRACT

A ricochet model for long rods developed by the author has been revisited in search of solution efficiencies. By replacing a moment-of-momentum governing equation in the original model with a simpler minimization constraint, a solution technique has been developed that avoids the complexity of an iterative solution that characterized the original work. The revised model retains key elements of the original model, including: ricochet by way of plastic hinge formation; rod rebound from the target's ricochet surface; and target gouging as a means to redirect the target force's line of action. Finally, the ricochet equations are analytically rendered so as to give a keen sense of how the critical obliquity for ricochet varies as a function of the initial conditions of the ballistic engagement.

15. SUBJECT TERMS
ricochet, plastic hinge, analytical solution, long rod

16. SECURITY CLASSIFICATION OF:			17. LIMITATION OF ABSTRACT	18. NUMBER OF PAGES	19a. NAME OF RESPONSIBLE PERSON
a. REPORT	b. ABSTRACT	c. THIS PAGE			Steven B. Segletes
UNCLASSIFIED	UNCLASSIFIED	UNCLASSIFIED	UL	42	19b. TELEPHONE NUMBER (*Include area code*) 410-306-1939

Available online at www.sciencedirect.com
ScienceDirect
International Journal of Impact Engineering 34 (2007) 899–925
INTERNATIONAL JOURNAL OF IMPACT ENGINEERING
www.elsevier.com/locate/ijimpeng

Further development of a model for rod ricochet

Steven B. Segletes*

US Army Research Laboratory, Aberdeen Proving Ground, MD 21005-5069, USA

Received 12 September 2005; received in revised form 27 February 2006; accepted 6 March 2006
Available online 16 June 2006

Abstract

A ricochet model for long rods developed by the author has been revisited in search of solution efficiencies. By replacing a moment-of-momentum governing equation in the original model with a simpler minimization constraint, a solution technique has been developed that avoids the complexity of an iterative solution that characterized the original work. The revised model retains key elements of the original model, including: ricochet by way of plastic hinge formation; rod rebound from the target's ricochet surface; and target gouging as a means to redirect the target force's line of action. Finally, the ricochet equations are analytically rendered so as to give a keen sense of how the critical obliquity for ricochet varies as a function of the initial conditions of the ballistic engagement.

Keywords: Ricochet; Plastic hinge; Analytical solution; Long rod

1. Introduction

Recently, Segletes posited a model for rod ricochet [1,2] based on the notion that, during the ricochet event, a plastic hinge would form in the rod, remaining stationary with respect to the target, as rod material flowed into the hinge and turned through an angle so as to be directed away from a penetrating aspect. There is experimental evidence for this description of ricochet morphology, one example of which is shown in Fig. 1, [3].

For the model [1,2], the momentum equations for rod ricochet were derived, based upon the forces and moments acting upon and fluxes moving through a control volume that encompassed the plastic hinge, as described in Fig. 2. By assuming that the incompressible rod's cross-sectional area remains unchanged through the course of the ricochet, continuity dictates that the rod's velocity get redirected but remain unchanged in magnitude (V) within and upon exiting the plastic hinge. By inferring velocities directly from Fig. 1 measurements, this assumption of constant V can be shown as excellent for glancing obliquity. However, its validity is expected to diminish as the striking obliquity becomes more normal. Nonetheless, the assumption is retained for all impact conditions to facilitate analytical solution. Expressing the equations for linear momentum perpendicular to the rod axis and target-force's line of action,

*Tel.: +1 410 306 1939; fax: +1 410 306 0783.
E-mail address: steven@arl.army.mil.

0734-743X/$ - see front matter © 2006 Elsevier Ltd. All rights reserved.
doi:10.1016/j.ijimpeng.2006.03.004

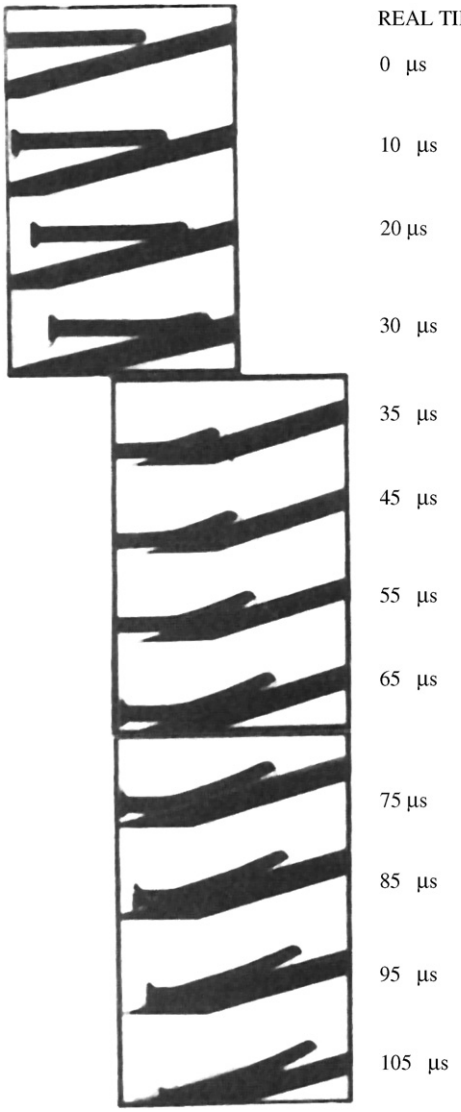

Fig. 1. Spark cinematography of a ricocheting rod projectile, [3].

respectively, Segletes obtained

$$F\,\sin(\theta+\eta) = T + V\dot{m}\,\cos(\theta-\alpha), \tag{1}$$

$$f\,\sin(\theta+\eta) = T\,\cos(\theta+\eta) + V\dot{m}[\cos(\alpha+\eta) - \sin(\theta+\eta)], \tag{2}$$

where θ is the impact obliquity as measured from the target normal, α is the angle of projectile rebound as measured between the target surface and the trajectory of the ricocheting rod, η is the angle between the target normal and the line of action of the force exerted by the target (positive when the line of action moves away from the rod's initial trajectory), F is the force applied by the target to the plastic hinge, f is the net axial compression force in the rod that is applied to the hinge, T is the shear traction applied by the cross-section of the rod to the plastic hinge, and $\mathrm{d}m/\mathrm{d}t$ is the rate of mass flow of rod material through the plastic hinge. By assuming a frictionless interface between rod and target, $\eta = 0$ for those cases where the target remains elastic during the ricochet. Only when the target is plastically gouged during ricochet will the resultant crater allow

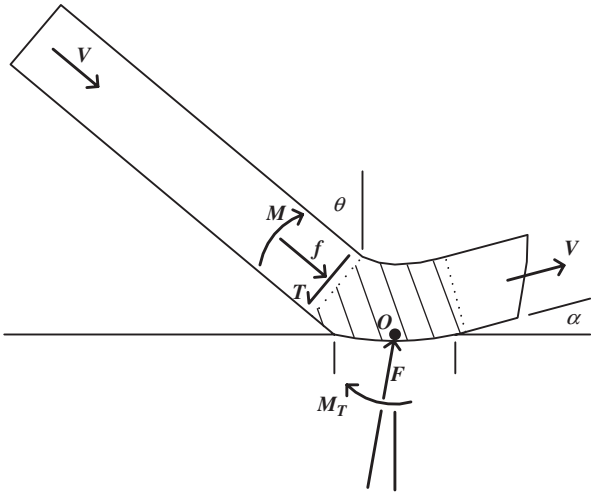

Fig. 2. A macro-view of ricochet phenomenology, depicting forces and moments upon and fluxes through the plastic hinge contained within the shaded control volume of the rod [1].

the target force's line of action to be directed at a nonzero angle η with respect to the target normal. In essence, the angle η represents an angular declination of the effective rod/target bearing surface with respect to the target plane.

The notion of a plastic hinge would seem to limit the model's applicability to ductile rods. However, the model assumes, as revealed in Fig. 2, that that ricocheting material exiting the hinge region provides a stress-free boundary condition to the hinge's governing momentum equations. In this sense, regardless of whether the ricocheting material is intact rod (as in Fig. 1) or a spray of redirected fragments, the assumed stress-free boundary at the hinge's exit seems analytically defensible. And while the mechanics of ductile bending and brittle fracture are quite different, the equations being solved here are momentum equations, not solid-mechanics equations. There is thus reason to believe, as long as the material entering the hinge can support bending stress and the material leaving the hinge is stress free, that the modeling approach may retain validity even when the rod is brittle, where ricochet is accompanied by the fracture of the rod. In the case of a ricocheting spray of fragments, the model variable α would necessarily refer to a single momentum-averaged trajectory that characterizes the spray.

The magnitude of the momentum flux in any cross-section of the rod, is given as

$$V\dot{m} = \rho V^2 A_0, \tag{3}$$

where ρ is the density of the rod material, and A_0 is the cross-sectional area of the rod. The maximum axial force that the rod can sustain is

$$f_{\max} = YA_0, \tag{4}$$

where Y is the strength of the rod. Segletes introduced an "interaction ellipse" between rod and target by projecting the rod's cross-section upon the target surface. By further introducing the artifice of a flat "bearing surface" between rod and target, normal to the action of the target's applied force (i.e., canted by angle η with respect to the interaction ellipse), the maximum allowable force that the target could bear upon the plastic hinge of the rod was deduced as

$$F_{\max} = HA_0 \frac{\cos\eta}{\cos\theta}, \tag{5}$$

where H is the target's resistance to penetration.

Without further constraint, there is the possibility of many solutions to the momentum equations, Eqs. (1) and (2), through variation of the rod and target forces over the allowable domains. Segletes [1,2] adopted a moment-of-momentum balance as an additional governing equation to help constrain the problem. However, its introduction required a detailed specification of the stress fields acting upon the plastic hinge, and complicated the solution method greatly. Solutions to the system of equations were obtained through a computational approach involving significant iteration. In an effort to greatly simplify the approach, and remove the need for iterative solution methods, we herein choose to dispense with the moment-of-momentum balance, and replace it with a much simpler constraint requiring the minimization of the projectile's rebound angle α.

Such a minimization can be justified on two grounds: (1) the rate of plastic work in the deforming projectile is minimized (since minimizing the rebound angle likewise minimizes the plastic turning angle of the rod); and (2) the stress load upon the target and, by inference, the target's stored elastic energy are minimized during the ricochet.

2. Revised model development

Define the nondimensional parameters

$$A = \frac{H}{\rho V^2}, \tag{6}$$

$$B = \frac{Y}{\rho V^2} \tag{7}$$

and

$$\beta = 1 + B. \tag{8}$$

The parameters A, B, and β are governed by the material properties of the rod (ρ, Y), the target (H), and the speed of the impact (V). Note that, in light of Eqs. (3)–(5) and these definitions, $A = (F_{\max}/V\dot{m}) \cdot (\cos\theta/\cos\eta)$ and $B = f_{\max}/V\dot{m}$. One may also define an effective value of A, call it a, which can be employed to represent the actual target force during ricochet, F, relative to the maximum allowed target force, as $a/A = F/F_{\max}$. Correspondingly for the rod, one may define an effective value of B, call it b, in terms of the actual net and maximum permissible rod forces, as $b/B = f/f_{\max}$. Likewise, let $\beta_{\text{eff}} = 1 + b$.

For cases where target gouging occurs during ricochet, the target force F is necessarily at its maximum allowable (i.e., plastic) value, $F_{\max}$. Thus,

Target force constraint:

$$\begin{aligned} &0 < a \leqslant A,\ \eta = 0 \text{ (elastic target)},\\ &a = A,\ \eta \neq 0 \text{ (plastic target)}. \end{aligned} \tag{9}$$

The rod, however, will always be plastic in the bending hinge, while the net compressive force imparted by the rod at the hinge will depend on the location of the neutral stress fiber in the plastic hinge. For example, if the neutral fiber of the hinge exactly traverses the centroid of the rod's cross-section, the rod will be in a state of pure bending, and f will be zero (even as the rod is yielding, bending, and ricocheting), such that β_{eff} will identically equal unity. Constraining the rod to a non-tensile state between pure bending and pure compression gives:

Rod-hinge force constraint:

$$1 \leqslant \beta_{\text{eff}} \leqslant \beta. \tag{10}$$

The original momentum equations, Eqs. (1)–(2), when shear stresses are ignored in the rod (i.e., when $T = 0$), may be expressed, via direct substitution, as

Governing momentum equations:

$$a = \frac{\cos(\theta - \alpha)}{\sin(\theta + \eta)} \frac{\cos\,\theta}{\cos\,\eta} \tag{11}$$

and

$$\beta_{\text{eff}} = \frac{\cos(\alpha + \eta)}{\sin(\theta + \eta)}. \tag{12}$$

Failure to consider the possibility of shear stresses in the rod, in the development of Eqs. (11)–(12), is a regrettable necessity to facilitate the solution pursued in this article. However, a mitigating factor in this assumption is that the shear traction T must, from kinematic arguments, take on a positive magnitude, using the convention of Fig. 2. A positive value of T works against the actions of both F in Eq. (1) and f in Eq. (2), implying that target stresses and the axial rod force must increase to compensate for any non-trivial value of T. While there exists one very limited circumstance in which this situation could be helpful (i.e., when a negative f would otherwise be needed to facilitate a ricochet solution), the introduction of shear traction T, in general, works against the viability of ricochet solution.

Quite simply then, with the omission of the moment-of-momentum equation, the remainder of this report is directed to the analytical solution of the system given by Eqs. (11)–(12). In addition to the force constraints, Eqs. (9)–(10), a list of kinematic constraints currently employed is given below, including rebound minimization and those developed previously [1,2] that still apply to the revised approach.

3. Kinematic ricochet constraints

(1) *Ricochet definition criterion:* ricochet is defined as when the trajectory of an impacting rod rebounds away from (i.e., bounces off) the surface plane of the target or, in the limit, is redirected along a trajectory of grazing incidence. Using the current nomenclature, $\alpha \geqslant 0$.

(2) *Plastic-hinge turning-limit criterion:* a tenet of the ricochet solution is that the rod may not, by way of plastic hinge, turn through an angle greater than $\pi/2$. The argument for this criterion is that a penetrator-dwell event would be kinematically more likely vis-à-vis an obtuse flow-turning, given that the stresses developed in turning a rod through an angle greater than $\pi/2$ would exceed the stagnation stresses of the dwell alternative. This criterion translates to the statement $\alpha \leqslant \theta$. Thus, in any valid ricochet solution, the maximum permissible value of α is θ.

(3) *Reflection-angle limit criterion:* given that η represents the angular declination of the bearing surface relative to the target plane, the criterion that limits the angle of reflection, $(\alpha+\eta)$, to an angle less than or equal the angle of incidence, $(\pi/2-\theta-\eta)$, follows as $\alpha \leqslant \pi/2-\theta-2\eta$. This criterion supersedes the one posited in the prior model [1,2], which failed to account for the declination of the bearing surface in evaluating the angles of incidence and reflection. By starting with Eq. (12) and substituting $\sin(\pi/2-\alpha-\eta)$ for $\cos(\alpha+\eta)$, this reflection-angle limit criterion may be shown equivalent to a subset of Eq. (10), requiring that $\beta_{\text{eff}} \geqslant 1$ (i.e., that the impacting rod not be in a state of net tension).

(4) *Gouge-geometry criterion:* based on arguments [1,2] using Fig. 3, it was shown that, for any symmetric ricochet gouge whose lip forms an angle ξ with respect to the target surface, the line of action of the target force, defined by η, and the rebound angle α, were constrained by the gouge geometry in such a way that $|\eta| \leqslant \alpha$ is a requirement (the argument concluded that $\alpha \geqslant \xi$ and $\xi \geqslant |\eta|$ simultaneously, leading to the constraint). While solutions with negative η are viable, an elastic solution (in which $\eta = 0$) may always be obtained in such cases. Thus, for practical purposes, $\eta \geqslant 0$ always and the gouge-geometry criterion, in application, simplifies to $0 \leqslant \eta \leqslant \alpha$.

(5) *Rebound minimization criterion:* the additional constraint which will serve to define a unique solution to the momentum equations (and which replaces the moment-of-momentum constraint utilized in the earlier model [1,2]) is that the rebound angle α is to be minimized (subject to the definition of ricochet that $\alpha \geqslant 0$). As previously stated, this minimization constraint has the effect of minimizing both the rate of plastic work in the ricocheting rod as well as the stored elastic energy in the target, during the event. However, and like the prior methodology, the elastic target ($\eta = 0$) solution space is exhausted before considering gouging solutions

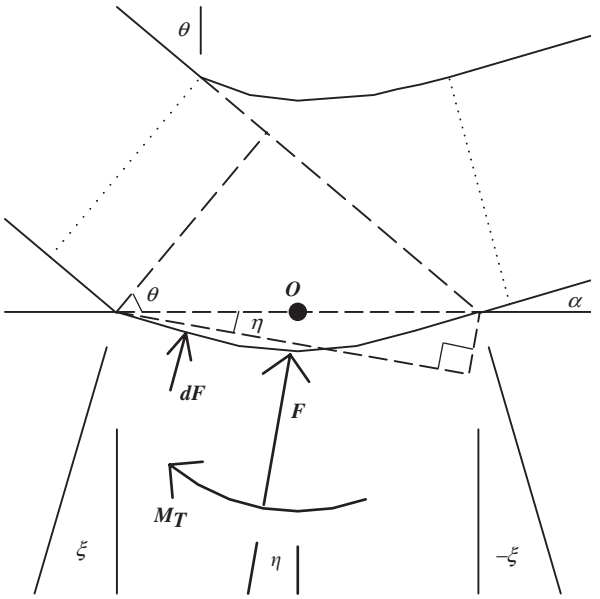

Fig. 3. Geometrical underpinnings of the $|\eta| \leqslant \alpha$ constraint [1].

involving non-trivial values of η, even though there may exist certain cases in which a gouging solution produces a smaller rebound angle than the corresponding elastic-target solution. It will be shown, for a given choice of A and θ, that to choose an otherwise viable solution with the smallest α is equivalent to choosing the viable solution with the largest β_{eff}.

4. Elastic ricochet

The case of elastic ricochet (i.e., for which the target remains elastic) presents a simplified form of the general ricochet problem. While the target force, embodied in variable a, is known in advance only insofar as the bounds $0 < a \leqslant A$, the definitional knowledge that $\eta = 0$ for elastic ricochet greatly simplifies the governing momentum equations. Derivations for the elastic- and other special-case solutions are outlined in Appendix A. Here, only final results are presented. These results follow from Eqs. (9)–(12), subject to the various kinematic constraints.

The basic morphology of elastic ricochet is that, if the striking obliquity angle θ is large enough, the trajectory of the incoming rod may be redirected with the minimum flow turning to a grazing incidence parallel with the surface of the target (i.e., there is no rebound of the ricocheted rod from the target surface and $\alpha = 0$ as a result). In these cases, the rod turns through an angle of $\pi/2 - \theta$ within the plastic hinge. Eventually, as the striking incidence θ is decreased towards the normal, there comes a point at which either the target strength can no longer sustain the increasing load associated with the momentum flux of the incoming rod, or else the rod's strength can no longer sustain the large momentum flux associated with the ricocheted rod. This limiting obliquity at which zero rebound, α, still persists is designated as $\theta_{\alpha=0}$.

Segletes [1,2], in an early attempt to simplify the calculation of ricochet, actually solved and presented this very restrictive $\alpha = 0$ ricochet result as a "simplified model." Using the nomenclature of the present article, the simplified ricochet criterion was given as

$$\sin \theta_{\alpha=0} = \max\left[-A/2 + \sqrt{1 + (A/2)^2}, 1/\beta\right]. \tag{13}$$

For some cases, however, the elastic-ricochet event can be prolonged to lower θ if the penetrator responds by rebounding off the target surface. The rebound angle, α, increases as θ is successively decreased until some critical angle of elastic ricochet, θ_c^e, below which elastic ricochet is no longer possible. At this critical level of

ricochet, the rebound has reached its maximum elastic value, $\theta^{\mathrm{e}}_{\max}$. For intermediate values of impact obliquity $\theta^{\mathrm{e}}_{\mathrm{c}} \leqslant \theta \leqslant \theta_{\alpha=0}$, the rebound falls in the range $\theta^{\mathrm{e}}_{\max} \geqslant \alpha \geqslant 0$. Altogether, in the solution of the equations for elastic ricochet, there are three branches of behavior that comprise the solution.

In what is called "branch I," it is the target strength, embodied in A, that is the limiting factor which prevents continued ricochet as the impact obliquity θ is lowered. Furthermore, in this branch of ricochet behavior, the problem cannot be remedied by way of an increased rebound angle α, since any increase in α comes at the cost of an increased target stress. For branch I elastic ricochet, the obliquity limit for $\alpha = 0$ ricochet, is identical to the critical angle for elastic ricochet, and there is no rebound in this branch of elastic ricochet:

Elastic ricochet branch I: $A < \beta - 1/\beta$

$$\theta_{\alpha=0} = \sin^{-1}\left[-A/2 + \sqrt{1 + (A/2)^2}\right], \tag{14}$$

$$\theta^{\mathrm{e}}_{\mathrm{c}} = \theta_{\alpha=0}, \tag{15}$$

$$\alpha^{\mathrm{e}}_{\max} = 0, \tag{16}$$

At $\theta = \theta^{\mathrm{e}}_{\mathrm{c}} : f < f_{\max}$ and $F = F_{\max}$.

At the other extreme, designated "branch III" elastic ricochet, it is the rod strength which limits the non-rebounding elastic ricochet. However, in this solution branch, the critical ricochet angle may be lowered below the $\alpha = 0$ non-rebounding limit, thereby inducing the rod to rebound from the target surface. As the rod trajectory changes in the form of increasing rebound, in response to a lowering of the striking obliquity, an increasing fraction of the rebounding rod's momentum flux is borne as load by the elastic target. Assuming that the target strength can elastically sustain this increase of load, this compensating process can continue with decreasing striking obliquity θ until the plastic-hinge turning-limit criterion is reached:

Elastic ricochet branch III: $A > \beta$

$$\theta_{\alpha=0} = \sin^{-1}(1/\beta), \tag{17}$$

$$\theta^{\mathrm{e}}_{\mathrm{c}} = \tan^{-1}(1/\beta), \tag{18}$$

$$\alpha^{\mathrm{e}}_{\max} = \theta^{\mathrm{e}}_{\mathrm{c}}, \tag{19}$$

For $\theta^{e}_{c} \leqslant \theta \leqslant \theta_{\alpha=0} : \alpha = \cos^{-1}(\beta \sin \theta)$, $f = f_{\max}$ and $FF_{\max}$.

Between these two extreme branches of target-limited and rod-limited ricochet, "branch II" elastic ricochet defines the region where, initially, it is the rod's strength which limits the obliquity of non-rebounding ricochet. However, as the striking obliquity is further lowered, accompanied by increasing rod rebound, the increased target load associated with the rebound eventually pushes the target to its limit force, thereby limiting the obliquity for elastic ricochet:

Elastic ricochet branch II: $\beta - 1/\beta \leqslant A \leqslant \beta$

$$\theta_{\alpha=0} = \sin^{-1}(1/\beta), \tag{20}$$

$$\theta^{\mathrm{e}}_{\mathrm{c}} = \cos^{-1}\left(A \Big/ \sqrt{1 + 2A\beta - \beta^2}\right), \tag{21}$$

$$\alpha^{\mathrm{e}}_{\max} = \cos^{-1}(\beta \sin \theta^{\mathrm{e}}_{\mathrm{c}}), \tag{22}$$

For $\theta^{\mathrm{e}}_{\mathrm{c}} \theta \leqslant \theta_{\alpha=0} : \alpha = \cos^{-1}(\beta \sin \theta)$, $f = f_{\max}$, and $FF_{\max}$.

At $\theta = \theta^{e}_{c} : f = f_{\max}$ and $F = F_{\max}$.

The domain of engagement scenarios over which these three branches of elastic ricochet operate is depicted in Fig. 4. Therefore, given a particular ballistic engagement scenario, one may ascertain which branch of elastic ricochet is potentially operational. Once the elastic-ricochet branch has been determined, the particular

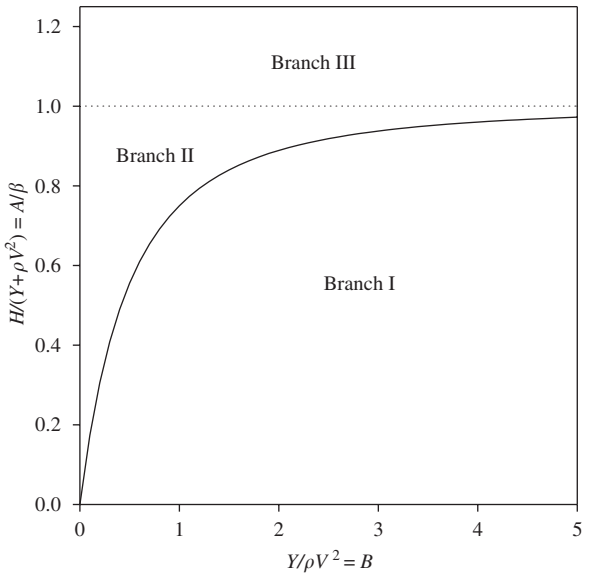

Fig. 4. Branches of elastic ricochet, depicted as a function of rod and target material properties.

values for $\theta_{\alpha=0}$ and θ_c^e may be calculated for that branch, and compared with the actual engagement obliquity to determine whether the elastic-ricochet conditions are met. If so, all that is left is to determine the rebound angle from Eqs. (16), (19), or (22), respectively. The calculation is complete and need go no further. Only if the engagement obliquity falls below the critical value for elastic ricochet need further consideration be given. In this case, ricochet involving target plasticity (in the form of target gouging) needs to be considered as a possibility. The next section on plastic ricochet details how this is done.

5. Plastic ricochet

Below are given the solutions to various special-case conditions, which will be used to ascertain the more general solution for plastic ricochet. For all special cases, one may assume that the following material and initial conditions are known (i.e., fixed): A, B (i.e., β), and θ. The unknowns, one or more of which are defined by each particular special case being considered, are η, α, and β_{eff} (i.e., b). Because the target is known to be plastic, it is known in advance that $a=A$. These special case solutions are not, in and of themselves, guaranteed to satisfy all the necessary constraints of ricochet. However, a judicious examination of the constraints in concert with the various special-case solutions will permit, if it exists, a general solution to be established that satisfies all the constraints. To assist the reader in deriving the final results given below, derivation strategies for these special-case solutions are given in Appendix A. These results follow from Eqs. (9)–(12), subject to the various kinematic constraints.

5.1. Solution for a specified β_{eff}

When a value for β_{eff} is directly specified, a solution for the governing momentum equations may be obtained as

$$\eta_{\beta\text{eff}} = \frac{1}{2}\sin^{-1}\frac{-pq - r\sqrt{r^2+p^2-q^2}}{r^2+p^2}, \tag{23}$$

where

$$q = A^2/2 - (\beta_{\text{eff}}A + 1 - \beta_{\text{eff}}^2)\cos^2\theta, \tag{24}$$

$$r = A^2/2 - \beta_{\text{eff}}A\cos^2\theta \tag{25}$$

and

$$p = \beta_{\text{eff}} A \sin\theta \cos\theta. \tag{26}$$

Note that, while negative η solutions are valid, they will never prevail, because there is always an elastic ($\eta = 0$) ricochet solution at equal or lesser value of β_{eff}. The associated value of α is given as

$$\alpha_{\beta\text{eff}} = \theta - \sin^{-1}[\beta_{\text{eff}} - A\cos(\theta + \eta_{\beta\text{eff}})\cos\eta_{\beta\text{eff}}/\cos\theta]. \tag{27}$$

5.2. Solution for which $\alpha = 0$

It may be shown that an $\alpha = 0$ solution to the governing momentum equations exists if

$$\frac{2 - A}{2\sin\theta} \leqslant 1 \text{ (if } \alpha = 0 \text{ solution exists)} \tag{28}$$

is satisfied by the material properties and initial conditions of impact. The value of η when Eq. (28) is satisfied is given by

$$\eta_{\alpha=0} = \frac{1}{2}\sin^{-1}\left[\frac{2\cos^3\theta}{A} - \frac{\sin 2\theta}{2}\left(1 + \sqrt{1 + \frac{4\sin\theta}{A} - \frac{4\cos^2\theta}{A^2}}\right)\right]. \tag{29}$$

The value of β_{eff} that satisfies this condition is

$$\beta_{\alpha=0} = \frac{\cos\eta_{\alpha=0}}{\sin(\theta + \eta_{\alpha=0})}. \tag{30}$$

Should Eq. (28) remain unsatisfied, no ricochet is possible, as it can be shown that, for such a condition, there will exist no solutions for which $0 \leqslant \alpha \leqslant \theta$.

5.3. Solution that maximizes α

Based on the plastic-hinge turning-limit criterion, the maximum permissible value for α is θ. An $\alpha = \theta$ solution, which represents $\alpha_{\max}$, is obtainable if

$$\frac{4 - A^2}{4A\tan\theta} \leqslant 1 \text{ (for } \alpha = \theta \text{ solution to exist)} \tag{31}$$

is satisfied by the initial conditions of the problem. The value of η when Eq. (31) can be satisfied is given by

$$\eta_{\alpha=\theta} = \frac{1}{2}\sin^{-1}\left[\frac{2\cos^2\theta}{A} - \frac{\sin 2\theta}{2}\left(1 + \sqrt{1 + \frac{4\tan\theta}{A} - \frac{4}{A^2}}\right)\right]. \tag{32}$$

The value of β_{eff} that satisfies this condition is

$$\beta_{\alpha=\theta} = \frac{1}{\tan(\theta + \eta_{\alpha=\theta})}. \tag{33}$$

Should Eq. (31) remain unsatisfied, however, there will be no solution for which $\alpha = \theta$. Nonetheless, a solution may be obtained which maximizes α (while keeping $\alpha < \theta$) by minimizing $\theta - \alpha$. In such cases, it may be shown that

$$\eta_{(\theta-\alpha)\min} = \pi/4 - \theta/2. \tag{34}$$

It is useful to define a quantity k as the cosine of this minimized ($\theta - \alpha$) angle. From this definition, it follows that

$$\alpha_{\max} = \theta - \cos^{-1} k, \tag{35}$$

where it can be shown that

$$k = \cos(\theta - \alpha)_{\min} = \frac{A}{2}\frac{(1 + \sin\theta)}{\cos\theta}. \tag{36}$$

The value of β_{eff} satisfying this condition is

$$\beta_{(\theta-\alpha)\,\min} = \sqrt{1-k^2} + A/2. \tag{37}$$

5.4. Solution for which $\alpha = \eta$

Based on the gouge-geometry criterion, $\eta \leqslant \alpha$, it is useful to know the conditions that provide a solution to Eqs. (11)–(12) for the limiting case of $\eta = \alpha$. The solution for this case may be reduced to a fourth-order polynomial in $\tan\eta$, as

$$0 = \tan^4\eta_{\alpha=\eta} + \frac{2}{\tan\theta}\tan^3\eta_{\alpha=\eta} + \frac{1-A^2}{\sin^2\theta}\tan^2\eta_{\alpha=\eta} + \frac{4(\cos^2\theta - A^2)}{\sin 2\theta}\tan\eta_{\alpha=\eta} + \left(\frac{1}{\tan^2\theta} - \frac{A^2}{\cos^2\theta}\right). \tag{38}$$

Standard analytical methods [4] may be applied to Eq. (38), so as to obtain the roots to this quartic polynomial in a direct fashion. Of the four solutions obtained, the smallest, positive, real solution for $\tan\eta_{\alpha=\eta}$ is the one desired, if it exists. Thus,

$$\eta_{\alpha=\eta} = \tan^{-1}[\text{smallest, positive, real solution to Eq. (38)}].$$

While solving Eq. (38) for the case of very large A values (e.g., very slow impacts which, nonetheless, deform the target plastically while forming a plastic hinge in the rod) is not of particular ballistic interest, it should be noted for completeness that experience reveals that, even in double-precision arithmetic, errors of precision in the analytical solution can produce unacceptable results in which valid ricochet scenarios are not evaluated as such. It may be tempting simply to address the issue by realizing that valid plastic-ricochet scenarios for large A can only occur at very small values of θ (large θ situations are elastic) and that, for very small θ, the value of $\cos\theta \sim 1$. In such cases, from Eq. (11), it is deduced that η is nearly independent of β_{eff} (and α), with a limiting value of

$$\eta_{A\gg 1} \to \sin^{-1}(1/A) - \theta. \tag{39}$$

However, a slightly more accurate approximate solution to the $\alpha = \eta$ problem may be obtained, solving Eq. (11) for large A, by first assuming that α may be approximated by η^*, where η^* is a known value of η is the vicinity of the $\alpha = \eta$ solution being sought. Because the behavior of η is nearly constant with β_{eff} for large A, this approximation is very good. Eliminating α thus from Eq. (11) permits the solution to be reduced from a quartic to a quadratic equation, the result being

$$\eta_{\alpha=\eta} = \frac{1}{2}\sin^{-1}\left[\tan\theta\cos^2\theta\left(E - 1 - \sqrt{E(2-E)\tan^2\theta + 1}\right)\right] \text{ (for large } A\text{)}, \tag{40}$$

where

$$E = \frac{2\cos(\theta-\eta^*)}{A\tan\theta}. \tag{41}$$

In the actual implementation of the general solution algorithm, when this large-A difficulty is detected, it is convenient to use the value $\eta^* = \eta_{\alpha\ \max}$, though this is by no means the only possibility. Once $\eta_{\alpha=\eta}$ is obtained thus, α is reset to this value from its earlier η^* approximation.

Finally, regardless of the method by which $\eta_{\alpha=\eta}$ is obtained, the associated β is given as

$$\beta_{\alpha=\eta} = \frac{\cos(2\eta_{\alpha=\eta})}{\sin(\theta+\eta_{\alpha=\eta})}. \tag{42}$$

5.5. Solution for which $\eta = 0$

In a like manner, the momentum equations may be solved for the special condition of $\eta = 0$, to yield

$$\beta_{\eta=0} = A + \sqrt{1 - (A \tan\theta)^2}, \tag{43}$$

$$\alpha_{\eta=0} = \theta - \cos^{-1}(A \tan\theta). \tag{44}$$

Of course, it follows that the solution for this condition exists only when $A \tan\theta \leqslant 1$.

6. General-solution strategy

The special-case plastic-ricochet solutions, Eqs. (23)–(44), show that there are many solutions which satisfy Eqs. (11)–(12). And so, while the elastic-ricochet solution is direct and straightforward to employ, the question naturally arises, in connection with the constraint to minimize α, how to select the proper ricochet solution when the target is no longer elastic.

To answer this question, two derivatives need to be established (keeping in mind that A and θ are fixed for this analysis). First, take Eq. (11) (which, for the plastic case, $a = A$) and differentiate with respect to η to obtain

$$\frac{d\alpha}{d\eta} = \frac{A\cos(\theta + 2\eta)}{\cos\theta \sin(\theta - \alpha)}. \tag{45}$$

Over the "domain of viable solutions," defined here as the solution space to Eqs. (11)–(12) in which the initial four kinematic constraints, embodied in the relation

$$0 \leqslant \eta \leqslant \alpha \leqslant \min[\theta, \pi/2 - \theta - 2\eta], \tag{46}$$

hold, it is clear from Eq. (45), in light of Eq. (46), that $d\alpha/d\eta > 0$. This means, within this domain of viable plastic solutions, that for any change in conditions that decreases η, α will likewise decrease, and vice versa. Next, take Eq. (12) and differentiate with respect to β_{eff} to obtain

$$\frac{d\eta}{d\beta_{\text{eff}}} = -\frac{\sin(\theta + \eta)}{\beta_{\text{eff}} \cos(\theta + \eta) + \sin(\alpha + \eta)(1 + d\alpha/d\eta)}. \tag{47}$$

Likewise, with all the individual terms on the right side being identifiable as positive, within the viable solution domain, it is clear that $d\eta/d\beta_{\text{eff}} < 0$.

What can be drawn from Eqs. (45) and (47) is that, when the viable solution domain (for fixed A and θ) is examined as a function of β_{eff}, both η and α must decrease with increasing β_{eff}. Therefore, the constraint of minimizing α translates into one of selecting the maximum value of β_{eff} within the domain of viable gouging-ricochet solutions.

For the case where an $\alpha = 0$ solution exists, via Eq. (28), for a given A, θ combination (since ricochet is otherwise precluded), Fig. 5 describes the four modes of behavior for α and η over the viable solution domain. The figure also includes a very rare variant of Mode IV behavior (deemed Mode IV-x) in which a double $\alpha = \eta$ crossover occurs. In each case, different logic must be applied in order to obtain the largest value of β_{eff} in the viable solution domain, and then guarantee that the solution simultaneously satisfies the rod-hinge force constraint, Eq. (10).

The algorithmic train of logic that will accomplish this task is described in Table 1. To summarize the logic in brief:

> If no elastic solution is viable, restrict the β_{eff} domain to the intersection of the material domain $[1, \beta]$ with the kinematic domain $[\beta_{\alpha\max}, \beta_{\alpha=0}]$; If the resultant β_{eff} domain is not the null set, pick the maximum β_{eff} in this domain for which $\eta \leqslant \alpha$, if such a value of β_{eff} exists.

Note, in the algorithm (and Fig. 5), that if the value of β, associated with $\alpha_{\max}$, would otherwise fall in the invalid [tensile] domain less than unity, the parameter $\alpha_{\max}$ is reset to the value associated with $\beta_{\text{eff}} = 1$. Furthermore, in the actual implementation of the algorithm, the $\eta = 0$ special solution is not

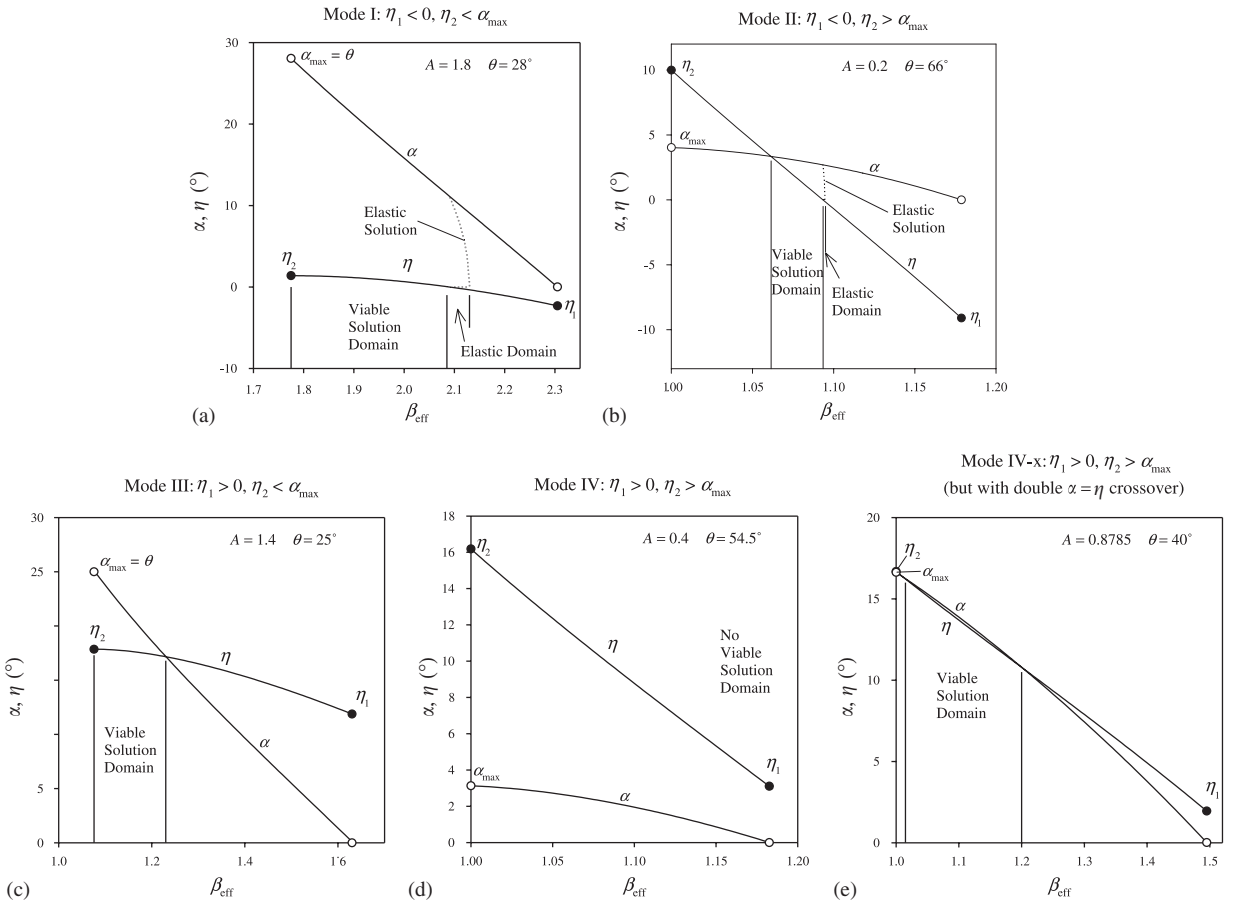

Fig. 5. Solution to the plastic ricochet equations, depicting four modes (and variant) of α, η behavior as a function of β_{eff} (note: $\eta_1 = \eta_{\alpha=0}$). Viable solution domain arises in regions where the kinematic constraints $0 \leqslant \alpha \leqslant \theta$, $\beta_{\text{eff}} \geqslant 1$, and $0 \leqslant \eta \leqslant \alpha$, simultaneously hold. Because it is desired to minimize α, the chosen solution will be the largest β_{eff} in the viable domain, subject to the rod-hinge force constraint, $\beta_{\text{eff}} \leqslant \beta$. Elastic solutions (shown in dotted lines) are always chosen in preference to plastic ones.

explicitly used to limit the viable solution domain for β_{eff}, because it is implicitly satisfied. For Modes I and II behavior, solutions that would otherwise satisfy the $\eta < 0$ condition would already have been discerned as elastic solutions, thus precluding the plastic algorithm's invocation. For Modes III and IV behavior, any $\eta < 0$ solution would have been otherwise ruled out by the $\beta_{\max}$ limiter associated with the $\alpha = 0$ criterion which, for these modes, is more stringent than the $\eta = 0$ criterion. Thus, while no coding is included to restrict the viable solution domain to positive η for plastic ricochet, the algorithm nonetheless assures it.

Upon ascertaining the values of α and η that satisfy the particular ricochet solution, the force quantities contributing to the ricochet are also of interest. Valid for situations involving either elastic or plastic ricochet, they reduce directly from the momentum equations, given the definitions of a and b, as

$$\frac{F}{F_{\max}} = \frac{a}{A} = \frac{1}{A} \cdot \frac{\cos(\theta - \alpha)}{\sin(\theta + \eta)} \frac{\cos\,\theta}{\cos\,\eta} \tag{48}$$

and

$$\frac{f}{f_{\max}} = \frac{b}{B} = \frac{1}{B} \cdot \left(\frac{\cos(\alpha + \eta)}{\sin(\theta + \eta)} - 1 \right). \tag{49}$$

Table 1
Ricochet algorithm logic

Generate elastic ricochet criteria, as a function of given A and β.
IF θ greater than the critical angle of elastic ricochet (i.e., if elastic solution viable), THEN
  Obtain elastic ricochet solution for α (keeping $\eta=0$)[a].
ELSE
  Check for PLASTIC ricochet solution as follows:
  IF A, θ combination does not permit $\alpha=0$ solutions, THEN
    No ricochet. Without $\alpha=0$ solution, all solutions are $\alpha<0$ (not valid).
  ELSE
    Initially set tentative viable solution domain, $[\beta_{min},\beta_{max}]$, to $[1,\beta]$.
    Obtain $\alpha=0$ solution (including $\beta_{\alpha=0}$ and $\eta_{\alpha=0}$). Set $\eta_1=\eta_{\alpha=0}$.
    Reduce β_{max}, if necessary, from β to $\beta_{\alpha=0}$.
    Obtain maximized α solution $[\alpha=\theta$ or $(\theta-\alpha)_{min}]$.
    IF $\beta_{\alpha=\theta}$ (or $\beta_{(\theta-\alpha)min}$) larger than β_{min}, THEN
      Raise β_{min} from 1 to $\beta_{\alpha=\theta}$ (or $\beta_{(\theta-\alpha)min}$), accordingly.
      Set η_2 to value of $\eta_{\alpha=\theta}$ (or $\eta_{(\theta-\alpha)min}$).
    ELSE
      Obtain solution for specified β_{eff} equal to $\beta_{min}=1$.
      Set η_2 to value of $\eta_{\beta min}$. Reset α_{max} to value of $\alpha_{\beta min}$.
    END IF
    IF there still exists a nontrivial domain of viable β_{eff}, $[\beta_{min},\beta_{max}]$, THEN
      Obtain largest β_{eff} in domain $[\beta_{min},\beta_{max}]$ for which $\eta_{eff}\leqslant\alpha_{eff}$, as follows:
      IF $\eta_1\leqslant 0$ (Modes I or II), THEN
        Obtain tentative ricochet solution, by specifying β_{eff} as β_{max}.
        IF $\eta_{eff}>\alpha_{eff}$ (i.e., β outside viable Mode II domain), THEN
          No ricochet. Max allowed β on wrong side of α,η crossover.
        END IF
      ELSE IF $\eta_2\leqslant\alpha_{max}$ (Mode III), THEN
        Obtain tentative ricochet solution at $\alpha=\eta$ crossover.
        IF $\beta_{\alpha=\eta}>\beta$ (i.e., β in middle of viable domain), THEN
          Specify $\beta_{eff}=\beta$ ricochet solution, to restrain $\beta_{eff}\leqslant\beta$.
        END IF
      ELSE
        IF $\alpha=\eta$ crossover nonetheless exists, THEN
          IF $\beta_{\alpha=\eta}\leqslant\beta$, THEN
            Mode IV-x solution at $\beta_{eff}=\beta_{\alpha=\eta}$.
          ELSE
            IF $\eta_\beta\leqslant\alpha_\beta$, THEN
              Mode IV-x solution at $\beta_{eff}=\beta$.
            ELSE
              No ricochet. Mode IV-x value of β too low.
            END IF
          END IF
        END IF
        No ricochet. Mode IV: η everywhere greater than α over domain of viable β.
      END IF
    ELSE
      No ricochet. Effective domain of viable β nonexistent.
    END IF
  END IF
END IF

[a]Critical ricochet-decision points are given in underlined text.

While it is not shown here, the same technique employed by Segletes [1,2] may be used to relate the relative rod force f/f_{max} to the location of the neutral fiber in the plastic hinge and hence to the strain field in the rod. Such knowledge, along with the rod's material characteristics, may inform an estimate of whether the ricocheting rod retains its integrity or breaks into a spray of ricocheting fragments.

7. Comparison with prior model formulation

It has been noted that the difference between the model derived herein and its predecessor [1,2] is in the replacement of a moment-of-momentum relation with a rebound-minimization constraint, adopted here so as to simplify the model and afford analytical solution to the governing equations.

Despite what might seem a significant change to the model, the reality is that the identical momentum equations, solved in both models, serve as the primary determining factor of ricochet behavior. One might expect, since the moment-of-momentum relation is a more limiting "equality constraint" than the "minimization constraint" that replaced it, that the current model permits a slightly larger solution space for ricochet. We see in Fig. 6, which depicts a model comparison by way of a ricochet phase diagram, that this is true. The engagement scenario depicted in this figure was a test case presented in the original report, in which a rod of density $2700\,\mathrm{kg/m^3}$ and strength $Y=1.2\,\mathrm{GPa}$ was impacted against a target of resistance $H=1.25\,\mathrm{GPa}$. Since the propensity to ricochet, as measured experimentally for other scenarios and reported in the prior work, was at least as great as any of the ricochet models (and frequently greater), the expanded ricochet domain of the current model is a further step in the right direction.

Additionally, since the current model employs a constraint that expressly adopts the solution which minimizes projectile rebound, one might anticipate that the current model will tend to produce ricochets with smaller values of α than the original model [1,2]. This too has been verified. For the simulation of Fig. 6, when the striking velocity is selected as $V=700\,\mathrm{m/s}$, the prior work reported modeled rebound angles approaching 28°, with the corresponding η values between 0° and 11°. In contrast, the current model for the same simulation parameters places both α and η between 0° and 14° over the domain of ricochet solutions.

For the two cases that were compared against experimental results in the original reports [1,2], the revised formulation of the current model predicts ricochet characteristics identical to the simple model of ARL-TR-3257 [1], for the case of the short L/D, brittle penetrator (B32), over the range of experimental data (Fig. 7). For the longer, $L/D=15$, 93% tungsten rod results, critical ricochet obliquities from the currently revised formulation are 2–6° lower than even the simplified form of the earlier model over the striking velocity range of 600–1200 m/s (where ricochet was experimentally observed), but still not quite to the critical obliquity level noted in the experiments (Fig. 8). The original work [1,2] may be consulted for specific details of the geometry and material characteristics of the engagements. In any event, the revised model presented here produces the most accurate prediction of ricochet of the several models studied, including those by Tate [5] and Rosenberg et al. [6].

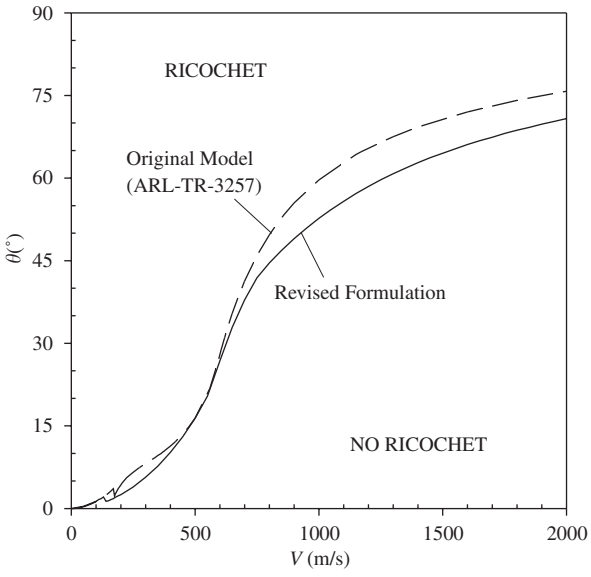

Fig. 6. Comparison of ricochet phase diagrams for engagement characterized by: $\rho=2700\,\mathrm{kg/m^3}$, $Y=1.2\,\mathrm{GPa}$, $H=1.25\,\mathrm{GPa}$.

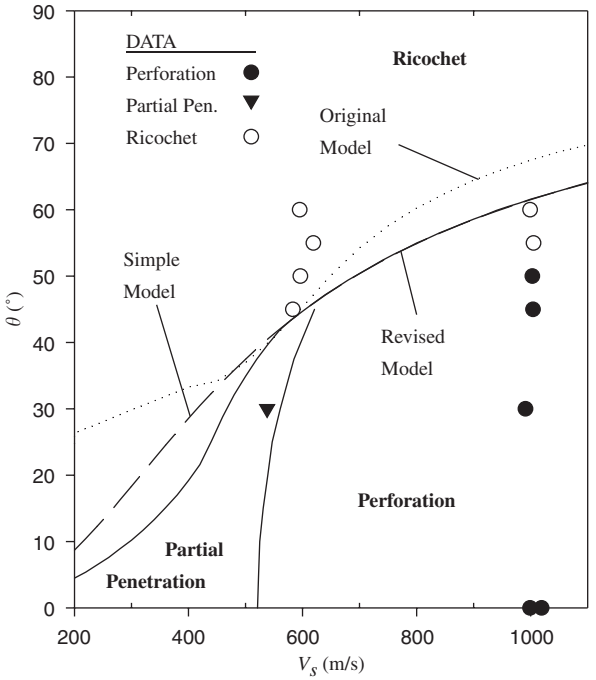

Fig. 7. Comparison of ricochet models for B32 penetration into aluminum (note: Tate and Rosenberg models predict no ricochet).

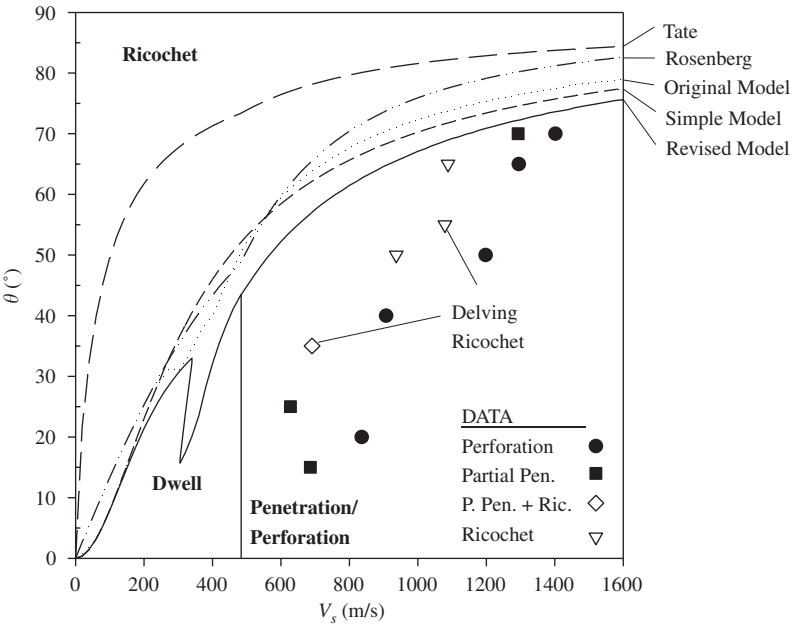

Fig. 8. Comparison of ricochet models to $L/D = 15$ tungsten alloy rods into aluminum.

8. Results of interest

In addition to comparing the revised formulation to the earlier model, it is interesting to explore the new formulation for its own sake. One point that should be noted is that, while most of the equations have been

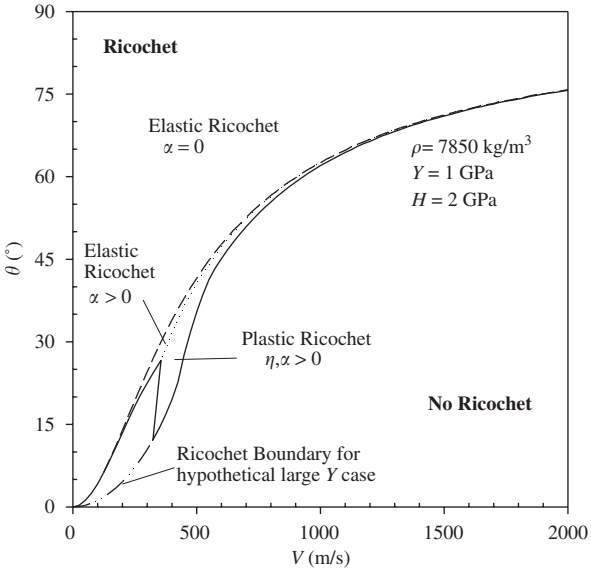

Fig. 9. Sample ricochet phase diagram for revised model.

devoted to solving the general problem of gouging ricochet, only a small portion of the V,θ engagement envelope is characterized by it. Fig. 9 shows this point clearly for a typical steel-on-steel engagement, where much of the diagram is either elastic $\alpha=0$ ricochet or, alternately, no-ricochet.

Also added on the graph is the reevaluated ricochet dividing line for a hypothetical case of a much stronger rod, which is shown to make several instructive points. First, the kink in the $Y=1$ GPa result at around 350 m/s impact velocity is clearly related to a limitation of the rod's strength to sustain ricochet, as this kink is absent for the "large Y case" curve. In fact, when ricochet occurs at low striking obliquities, the rod must necessarily turn approximately 90° during the ricochet, and travel with a correspondingly small rebound from the target surface. This means that the portion of rod momentum coming in to the plastic hinge can contribute virtually no force to balance the momentum flux leaving the hinge. Likewise, the target's force is nearly perpendicular to the flow of the ricocheted rod and can also contribute only a small component of its force to balance the ricocheted momentum flux. Therefore, a primary contributor to that flux balance (and what therefore is a limiting factor) must necessarily be the strength of the rod applied to the hinge.

While this explanation is supported by the equations, the predictions of ricochet at very low striking obliquities must be taken with some reservations, since they predict that a strengthened rod will be more likely to ricochet. Consider first, that the alternative to ricochet is not solely penetration, but might also include dwell (when the target resistance H exceeds the dynamic stress of the impacting rod, $Y+1/2\rho V^2$). In the example of Fig. 9, dwell would occur to a point beyond 500 m/s impact speed and so hypothetically strengthening the rod does not change the scenario from penetration to ricochet, but from dwell to ricochet, which is much more believable. Also, the whole basis of the present model is one that evaluates whether the rod and target strengths can *sustain* ricochet, not whether they can *initiate* it. Because it is known that ricochet is very nose-shape dependent, and that ricochet can not be sustained if it fails to initiate in the first place, the current model's underlying premise makes it ill suited to predict whether a strengthened rod would have initiated ricochet in the first place.

Another interesting behavior was observed that, at first glance, might seem counterintuitive. Recall from Fig. 5 and the associated discussion that α and η were determined to vary monotonically with increasing β_{eff}. Such monotonicity in β_{eff}, however, implies no such comparable behavior as a function of θ. Using the same material parameters of Fig. 9 and considering a specific impact speed of $V=400$ m/s, the variation of α and η are presented as a function of θ in Fig. 10. Recall that these curves do not represent purported behavior during a single impact, but that each chosen obliquity θ represents a unique ballistic engagement.

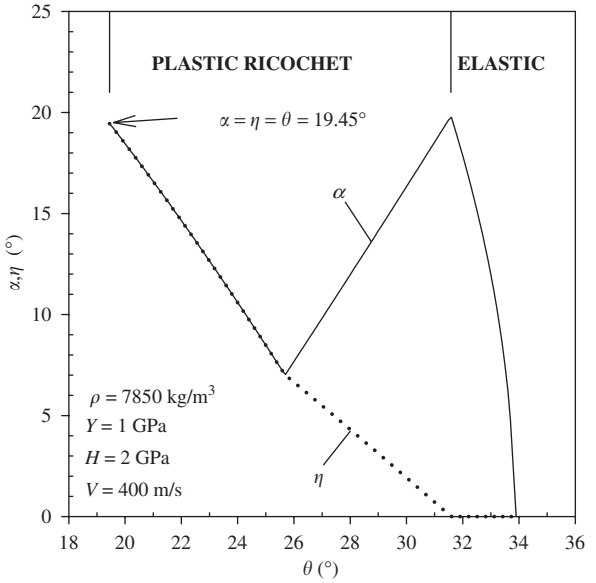

Fig. 10. Ricochet response of α and η as a function of striking obliquity.

While the fluctuation of α may seem erratic, each segment of behavior is understandable in terms of the constraints. As the striking obliquity is lowered to 33.9°, the rod strength becomes unable to sustain $\alpha = 0$ ricochet and starts to compensate with rod rebound off the elastic target. However, not only does lowering θ add load directly upon the target from the impacting portion of the rod, but the increasing rebound of the ricocheting rod further increases the target's load. When the target strength can longer sustain this load elastically (at a striking obliquity of 31.6°), it begins to gouge at impact.

The gouging allows the target to redirect its line of action by a few degrees in the direction of the ricocheting rod. This redirection of target force (an increasing η) provides a force component parallel with the target surface that allows the momentum flux of the ricocheting rod to be sustained at a lower value of rebound angle α. This mode of compensation (increasing η in exchange for decreasing α) proceeds as the striking obliquity is lowered, until the point at 25.7° striking obliquity where the value of η rises to meet that of the lowering α. At this point, the gouge lip has formed a 7° angle ξ with respect to the target surface (see Fig. 3). The target-force redirection η must be at an angle no greater than this gouge angle, while the rod rebound angle α must kinematically be at least as large as ξ. Thus, as the striking obliquity is further lowered, the target gouge deepens, which allows for an increasing η but only at the kinematic cost of increasing the rebound angle such that $\eta \leqslant \alpha$ is maintained.

Finally, as the obliquity is lowered to 19.45°, the rebound α, being forced upward by the deepening gouge, reaches this same level of 19.45°. At this point, the rod is making a 90° turn in direction from its striking orientation. The only way in which ricochet could be sustained at lower striking obliquity would be for the rod to continue turning in excess of 90°. However, such an adjustment is considered untenable, since the forces required to achieve this would exceed the forces required to dwell the penetrator. Thus, for impact obliquities below 19.45°, the more plausible scenario is that the rod would simply flatten and dwell upon the surface of the target, in the mode of a Taylor impact cylinder.

9. Critical ricochet obliquity relationships

To this point, all calculations, including those that portrayed a critical obliquity curve in one form or another, as in Figs. 6–9, were done by systematically applying the aforementioned general-solution strategy over the range of initial conditions considered. Such a method is necessary, if detailed ricochet response, such as that portrayed in Fig. 10, is sought. However, when all that is required is the minimum obliquity at which ricochet can possibly occur (i.e., the critical ricochet obliquity) for a specified combination of rod and target

material descriptions and impact velocity, it is desirable to have simpler relationships for making a quick assessment of ricochet likelihood. The development of such relationships would also serve to provide a heightened understanding of the ricochet phenomenon.

When the rod strength is large, it has been observed in the model that the critical angle of ricochet for low striking obliquity occurs when $\theta=\alpha=\eta$. Since the kinematic constraints require that $\eta\leqslant\alpha$ and $\alpha\leqslant\theta$, this $\theta=\alpha=\eta$ condition represents a clear limiting case for the critical ricochet angle. Based on the kinematic constraint that $\alpha\leqslant\pi/2-\theta-2\eta$, however, this condition can only occur at striking obliquities below $\theta\leqslant22.5^\circ$. Thus,

$$\alpha_c=\eta_c=\theta_c \text{ (when } \beta\geqslant\sqrt{A^2-1},\ 0\leqslant\theta_c\leqslant22.5^\circ), \tag{50}$$

where the β specification quantifies the rod-strength requirement. The critical obliquity for these conditions, from the momentum equations, may be derived as

$$\theta_c=\frac{1}{2}\sin^{-1}(1/A) \text{ (when } \beta\geqslant\sqrt{A^2-1},\ A\geqslant\sqrt{2}) \tag{51}$$

or, conversely,

$$A=\frac{1}{\sin\ 2\theta_c} \text{ (when } \beta\geqslant\sqrt{A^2-1},\ 0\leqslant0\leqslant22.5^\circ). \tag{52}$$

It is the simultaneous solution of Eq. (12), in light of Eq. (50) (i.e., $\beta\geqslant1/\tan2\theta_c$), with Eq. (52) that provides the constraint between A and β. The $\sqrt{2}$ limit on A corresponds to that value which will bring θ_c to 22.5°. It is exactly this curve which corresponds to the large-Y curve extension presented in Fig. 9. Correspondingly, it has been noted in the model that if the β constraint can not be satisfied for a given A in the range $A>\sqrt{2}$, then there are no plastic ricochet solutions, since all would-be plastic solutions violate the plastic-hinge turning-limit criterion. There will, however, be branch III (i.e., $A>\beta$) elastic solutions for $A>\sqrt{2}$, should the β requirement not be met for providing a plastic solution. However, these elastic solutions occur at higher values of striking obliquity, resulting in a jump in the θ_c curve.

In an adjacent range of critical plastic-ricochet obliquities, immediately above 22.5° for which $A<\sqrt{2}$, the limiting ricochet is governed by the gouge-geometry constraint and the reflection-angle-limit constraint which, taken at their limiting values, give $\alpha_c=\eta_c$ and $\alpha_c=\pi/2-\theta_c-2\eta_c$. The latter relation, in light of the former, reduces to

$$\alpha_c=\eta_c=30^\circ-\theta_c/3. \tag{53}$$

Furthermore, the reflection-angle limit constraint indicates that this condition must occur at a value of $\beta_{\text{eff}}=1$. These values of α_c, η_c and θ_c are then substituted into Eq. (11) in order to get the A value associated with that critical obliquity:

$$A=\frac{\cos\left((4\theta_c/3)-30^\circ\right)\cos\ \theta_c}{\sin\left((2\theta_c/3)+30^\circ\right)\cos\left((\theta_c/3)-30^\circ\right)}. \tag{54}$$

But through what obliquity beyond 22.5° will this condition prevail? From the aforementioned general-solution strategy, it is known that, when the solution departs from this condition, β_{eff} will increase beyond a value of unity, and α_c will diminish in comparison to the $[\beta_{\text{eff}}=1]$ value given by Eq. (53). Therefore, we conduct a perturbation analysis, in which we hypothesize a departure from this solution by allowing α_c to diminish by an infinitesimal amount ε:

$$\alpha_c=\eta_c=30^\circ-\theta_c/3-\varepsilon, \tag{55}$$

leading to

$$A=\frac{\cos\left((4\theta_c/3)-30^\circ+\varepsilon\right)\cos\ \theta_c}{\sin\left((2\theta_c/3)+30^\circ-\varepsilon\right)\cos\left((\theta_c/3-30^\circ+\varepsilon\right)}. \tag{56}$$

In order for this perturbation from the baseline solution to feasibly establish a lower critical ricochet angle (and thus an alternative to the baseline), $\partial\theta_c/\partial\varepsilon<0$ is required. Expressing this as $(\partial A/\partial\varepsilon)/(\partial A/\partial\theta_c)<0$, we note

that $\partial A/\partial\theta_c$ will be negative for all θ_c in the range $22.5^\circ<\theta_c\leqslant 90^\circ$, and so the feasibility of a departure from the $\beta_{\rm eff}=1$ solution hinges on the sign of $\partial A/\partial\varepsilon$ as $\varepsilon\to 0$. It may be shown that $\partial A/\partial\varepsilon$ changes sign in the limit $(\varepsilon\to 0)$ when the condition

$$\tan\left(\frac{4\theta_c}{3}-30^\circ\right)=\tan\left(\frac{\theta_c}{3}-30^\circ\right)+\cot\left(\frac{2\theta_c}{3}+30^\circ\right) \tag{57}$$

is met. This condition is met when $\theta_c=38.06^\circ$. Thus, the range on this $\beta_{\rm eff}=1$ solution spans $22.5^\circ<\theta_c\leqslant 38.06^\circ$, through which $\alpha_c=\eta_c=30^\circ-\theta_c/3$. From Eq. (54), it may be observed that the range on A for this region is $0.9373\leqslant A<\sqrt{2}$.

At larger θ_c, all the way to 90°, there continues to be a solution governed by the constraint $\alpha_c=\eta_c=30^\circ-\theta_c/3$, for $\beta_{\rm eff}=1$, though this particular solution is no longer that which minimizes α for cases of larger β. Nonetheless, for this very special $\beta_{\rm eff}=1$ case, Eq. (54) applies for relating A to θ_c. Further, it allows generalization over the range $38.06^\circ<\theta_c\leqslant 42.497^\circ$, corresponding to the range $0.8047\leqslant A<0.9373$. In this narrow range, for the A, θ_c pair given by the Eq. (54), there are two positive-η solutions for the $\alpha=\eta$ constrained momentum equations, i.e., for Eq. (38): the one given at $\beta_{\rm eff}=1$, and the other with $\beta_{\rm eff}$ in the range between 1 and 1.4803. For this second solution, the resulting value of $\alpha_c=\eta_c$ is smaller than the value for the $\beta_{\rm eff}=1$ solution, and is thus the preferable solution for ricochet.

It would be convenient to hope, for a given value of A, that when θ_c is lowered to the point where the $\beta=1$ solution disappears, that all the $\beta_{\rm eff}>1$ solutions would simultaneously disappear. Were that the case, then the $\beta=1$ solution, while not the preferable solution for ricochet, would still be indicative of the critical ricochet angle, θ_c. However, there is a slight imperfection with such a hypothesis, and that is the phenomenon of Mode IV-x ricochet depicted in Fig. 5e, in which the $\beta=1$ solution is no longer active, despite a range of intermediate β for which a ricochet solution does exist. This mode of solution can exist for striking obliquities greater than 38.06°, and will be discussed in more detail later. Suffice it to say, at this point, that the region where Mode IV-x ricochet can operate is a miniscule triangular region of the A,θ_c plane. Therefore, while not exact, Eq. (54), relating A to θ_c for the $\beta=1$ solution, provides an excellent approximation to the critical obliquity for $0.8047\leqslant A<0.9373$, for all $\beta\geqslant 1$.

A further difference between this solution and that for $22.5^\circ<\theta_c\leqslant 38.06^\circ$ is in the relationship for η_c and α_c. When $\beta=1$, the solution given by $\alpha_c=\eta_c=30^\circ-\theta_c/3$ still applies. However, when β is large enough, the preferable secondary solution applies, producing a lower magnitude of $\alpha_c=\eta_c$. When the value of β is in a range between these two solutions, the value for η_c will be less than that for α_c, yet both will fall in a range between the two $\alpha_c=\eta_c$ solutions. In either case, α_c is diminished with respect to the value associated with the $\beta=1$ solution.

The upper end of this range, associated with the A, θ_c pair of (0.8047, 42.497°), corresponds to that condition for which the secondary $\alpha_c=\eta_c$ solution is exactly $\alpha_c=\eta_c=0$, traditionally associated with an elastic Branch I solution. In fact, the upper end of the range was ascertained by equating the value of A for the $\beta_{\rm eff}=1$ plastic solution, Eq. (54), to that from the limiting $(a\to A)$ elastic Branch I solution, given by Eq. (11) with $\alpha=\eta=0$ and $a\to A$, such that

$$\frac{\cos^2\theta_c}{\sin\theta_c}=\frac{\cos\left((4\theta_c/3)-30^\circ\right)\cos\theta_c}{\sin\left((2\theta_c/3)+30^\circ\right)\cos\left((\theta_c/3)-30^\circ\right)}. \tag{58}$$

It is the solution of this equation which yields $\theta_c=42.497^\circ$, corresponding to $A=0.8047$. Thus, it is not surprising to suspect that, at obliquities in excess of 42.497°, elastic solutions may influence the critical obliquity.

Indeed, when ignoring the Mode IV-x solutions in the range of critical obliquities $\theta_c\geqslant 42.497^\circ$, the elastic Branch I criterion may govern the ricochet. When β exceeds the limit needed to force branch I elastic ricochet $(\alpha=0)$ in this range, by satisfying the relation $0.8047<\beta-1/\beta$ to yield $\beta>1.4803$, Eq. (11) becomes

$$A=\frac{\cos^2\theta_c^e}{\sin\theta_c^e}\ (\text{when } \beta>1.4803,\ \theta_c>42.497^\circ\ [\text{i.e., when } 0\leqslant A<0.8047]). \tag{59}$$

Table 2
Relations for critical ricochet obliquity

A, θ_c Range	Relation[a]	Restriction	η, α Behavior at θ_c
$A \geqslant 2^{1/2}$ $\theta_c \leqslant 22.5^\circ$ plastic, $\theta_c \leqslant 45^\circ$ elastic	$A = \dfrac{1}{\sin 2\theta_c}$	$\beta > \sqrt{A^2-1}$	$\alpha_c = \eta_c = \theta_c$
	Elastic: $\beta = \dfrac{1}{\tan\theta_c^e}$	$1 \leqslant \beta \leqslant \sqrt{A^2-1}$	$\eta = 0$, $\alpha = \theta_c$
$0.9373 \leqslant A < 2^{1/2}$ $22.5^\circ < \theta_c \leqslant 38.06^\circ$	$A = \dfrac{\cos\left((4\theta_c/3) - 30^\circ\right)\cos\theta_c}{\sin\left((2\theta_c/3) + 30^\circ\right)\cos\left((\theta_c/3) - 30^\circ\right)}$	all $\beta \geqslant 1$	$\alpha_c = \eta_c = 30^\circ - \theta_c/3$
$0.8047 \leqslant A < 0.9373$ $38.06^\circ < \theta_c \leqslant 42.497^\circ$	$A \approx \dfrac{\cos\left((4\theta_c/3) - 30^\circ\right)\cos\theta_c}{\sin\left((2\theta_c/3) + 30^\circ\right)\cos\left((\theta_c/3) - 30^\circ\right)}$	all $\beta \geqslant 1$	$0 \leqslant \eta_c \leqslant \alpha_c \leqslant 30^\circ - \theta_c/3$
$0 < A < 0.8047$ $\theta_c \geqslant 42.497^\circ$	$A_1 = \dfrac{\cos\left((4\theta_c/3) - 30^\circ\right)\cos\theta_c}{\sin\left((2\theta_c/3) + 30^\circ\right)\cos\left((\theta_c/3) - 30^\circ\right)}$	$\beta = 1$	$\alpha_c = \eta_c = 30^\circ - \theta_c/3$
	$A_2 \leqslant A \leqslant A_1$	$1 \leqslant \beta \leqslant 1.4803$	$0 \leqslant \eta_c \leqslant \alpha_c \leqslant 30^\circ - \theta_c/3$
	Elastic: $A_2 \approx \dfrac{\cos^2\theta_c^e}{\sin\theta_c^e}$ (relation is exact for $\theta_c \geqslant 45^\circ$)	$\beta > 1.4803$	$\alpha_c = \eta_c \approx 0$

[a]Relation specified is for plastic ricochet, unless otherwise noted. Also, the presence of Mode IV-x ricochet solutions makes some of the specified relations only approximate, denoted by the symbol $\approx$, instead of $=$.

Eq. (59), of course, can be inverted to yield the associated elastic-ricochet solution of Eq. (14):

$$\theta_c^e = \sin^{-1}\left[-A/2 + \sqrt{1 + (A/2)^2}\right] \text{ (when } \beta > 1.4803,\ \theta_c > 42.497^\circ \text{ [i.e., when } 0 \leqslant A < 0.8047\text{])}. \tag{60}$$

Once again ignoring the influence of Mode IV-x solutions, all solutions in this range will be bounded, as a function of β, between this elastic $\beta > 1.4803$ solution and the $\beta = 1$ plastic solution of Eqs. (53)–(54). Likewise, for this range of θ_c, the values of α_c and η_c will range between the values associated with the elastic and the $\beta = 1$ plastic solution. These elastic and plastic critical-obliquity functions are actually quite narrowly banded, producing critical obliquities within 3° of each other, for all $A < 0.8047$.

All of these relations described for critical ricochet are collated in Table 2, for convenience.

We return briefly to the situation of the Mode IV-x ricochet solutions which, when ignored, makes the described critical obliquity description an inexact one. The question to be answered is one of "how inexact?" Because the solution to the $\alpha = \eta$ condition, on which the Mode IV-x solutions depend, is a fourth-order equation, no simple description has yet been developed for the precise range over which this mode of solution may apply. However, through a systematic approach, the range of Mode IV-x solutions were obtained, in order to show the small degree to which they depart from the analytical descriptions otherwise put forth.

Fig. 11 documents the result. In the figure, solid lines of the graph denote the analytical functions presented here, while all dotted and/or dashed lines represent calculated quantities obtained through a systematic solution to the ricochet equations for specified values of θ, A, and β. It is easy to see how good a job the analytical description of critical ricochet obliquity angle does, even allowing for the Mode IV-x solutions. In all cases, the error in the predicted value of A for a given θ_c is always under 1.2%, and generally well under 1%. Mode IV-x ricochet plays a role in the critical obliquity only within the small triangular (A,θ_c) region delimited by the vertices $(1/\sqrt{2}, 45^\circ)$, $(0.9373, 38.06^\circ)$, and $(0.8047, 42.497^\circ)$. Further discussion on the intricacies of Mode IV-x ricochet is offered in Appendix B.

Fig. 12 summarizes the discussion of critical ricochet obliquity as a function of target parameter A. Note that the inclusion of plastic and elastic ricochet curves in this figure is not meant to denote a transition from one ricochet mode to another with increasing obliquity (though such transitions indeed happen). Rather, the

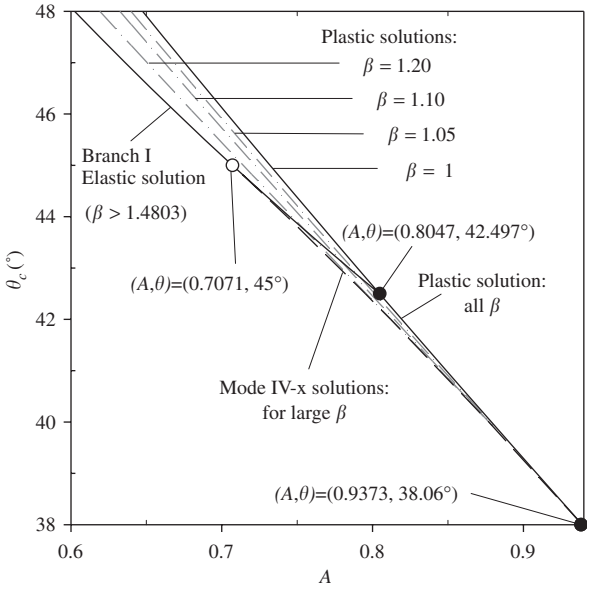

Fig. 11. The influence of Mode IV-x solutions on the calculation of critical ricochet obliquity. Solid lines represent the analytical functions given for plastic and elastic ricochet. Actual general-model behavior is depicted with dashed lines.

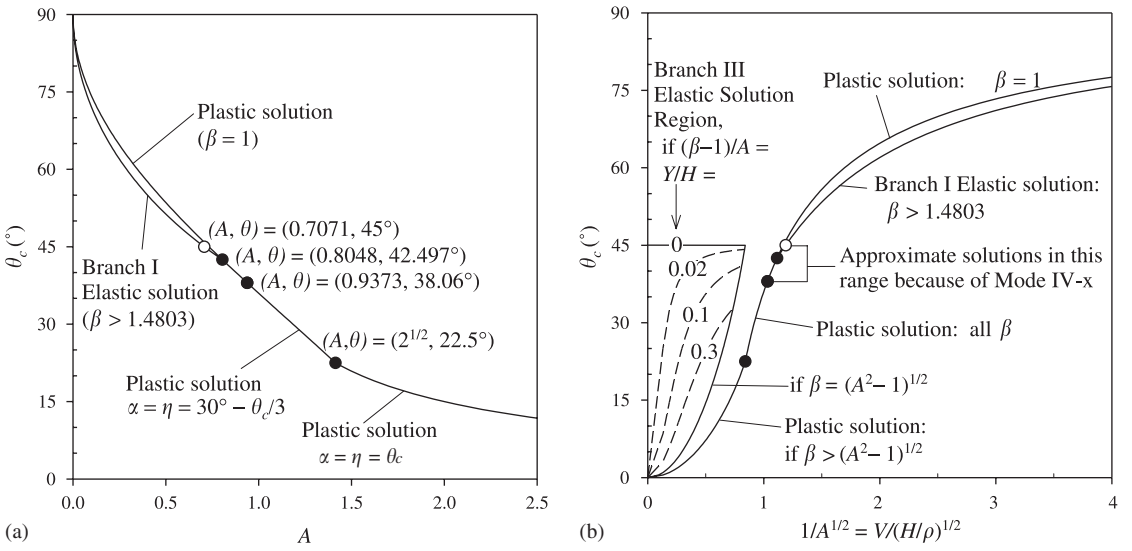

Fig. 12. Critical ricochet obliquity as a function of parameter A, showing the interplay of plastic and elastic solutions, based on value of β. Results are shown (a) for small values of A, and (b) as function of $1/A^{1/2}$.

multiplicity of curves is meant to show how the critical obliquity for ricochet can change as a function of the parameter β. In all cases, the curves are meant to denote the minimum obliquity at which ricochet can possibly occur as a function of A. In Fig. 12b, the graph is presented as a function of $1/A^{1/2}$, which is a parameter proportional to the striking velocity. The abrupt step between the $\beta > (A^2-1)^{1/2}$ plastic curve and the elastic $\beta = (A^2-1)^{1/2}$ curve is predicted by the model. According to the model, there can exist a "dead zone" of intermediary obliquities for which the conditions of neither elastic nor plastic ricochet is satisfied, resulting in the stepwise appearance seen, for example, in Fig. 9.

10. Conclusions

The long-rod ricochet algorithm posited by Segletes [1,2] has been revisited in search of efficiency improvements. The original method required an iterative approach to solving the equations of ricochet. One key step in accomplishing this improvement is the replacement of a moment-of-momentum governing equation in the original model with a simpler minimization constraint on the rebound angle of the ricocheting projectile.

With this change, the ricochet equations are now solved in analytical, non-iterative, form. For the case of elastic ricochet, there are three branches of ricochet behavior depending upon the relative magnitude of the target and projectile strengths, projectile density and striking velocity. The critical angle of elastic ricochet is quantifiable as a function of the elastic ricochet branch, so that a rapid assessment may be made of whether an elastic-ricochet solution presents itself. In the absence of an elastic ricochet solution, a non-iterative algorithm is employed to examine particular special-case plastic solutions so as to ascertain that solution which satisfies all the kinematic and force-limit constraints, including that for rebound minimization.

In the new algorithm, no iterative steps are required to obtain the ricochet determination/solution. As such, the current algorithm detailed in Table 1 offers a much more streamlined solution than that embodied in the original efforts [1,2]. Minor differences in results between the two methods are attributable to the replacement of the moment-of-momentum governing equation in the original work with the minimized-projectile-rebound-angle constraint in the current effort. Nonetheless, the revised model retains key elements of the original model, including: ricochet by way of plastic hinge formation; rod rebound from the target's ricochet surface; target gouging as a means to redirect the target force's line of action during the ricochet event; and, of course, linear-momentum conservation.

Analytical expressions are also offered for the critical ricochet obliquity as a function of the rod and target material descriptions and the striking velocity. These expressions are summarized in Table 2. In some engagement domains, the equations are exact solutions to the ricochet equations, while in other domains, the analytical expressions are very close approximations to the actual solution, acquired through the use of simplifying assumptions.

Appendix A. Derivation aid

The math presented in the article is solely based on solving the following system of equations:

Equation in A:

$$a = \frac{\cos(\theta-\alpha)}{\sin(\theta+\eta)}\frac{\cos\theta}{\cos\eta}, \tag{A.1}$$

Equation in β:

$$\beta_{\text{eff}} = \frac{\cos(\alpha+\eta)}{\sin(\theta+\eta)} \tag{A.2}$$

subject to the material constraints

$$0<a\leqslant A,\ \eta=0 \text{ (elastic target)}$$
$$a=A,\ \eta\neq 0 \text{ (plastic target)}$$
$$1\leqslant\beta_{\text{eff}}\leqslant\beta,$$

the kinematic constraints embodied in the relation

$$0\leqslant\eta\leqslant\alpha\leqslant\min[\theta,\pi/2-\theta-2\eta],$$

as well as the α-minimization constraint. The α-minimization constraint can be shown, for a given A and θ, to be equivalent to the solution that maximizes β_{eff}.

Derivation of key equations appearing in the article is herein described. One solution technique frequently used in this appendix involves the conversion of trigonometric terms to double angles, to eliminate sine–cosine

products. The identities

$$\cos^2\eta = (1+\cos 2\eta)/2 \tag{A.3}$$

and

$$\sin\eta\cos\eta = \sin 2\eta/2 \tag{A.4}$$

are employed to produce equations of the form $r\cos 2\eta + p\sin 2\eta + q = 0$. Isolating the cosine, squaring the equation, and converting the resulting $\cos^2\eta$ term to $1-\sin^2\eta$ produces a quadratic form in $\sin\eta$, allowing solution as

$$\sin 2\eta = \frac{-pq - r\sqrt{r^2+p^2-q^2}}{r^2+p^2}. \tag{A.5}$$

Note that only the minus root is retained, so as to keep $\eta<\theta$ for the range of η values to which this equation is applied in this article. The value of η is then obtained by way of an inverse sine. Specific special-case solutions are now addressed.

A.1. Elastic ricochet ($\eta=0$)

A.1.1. Branch I

In branch I, it is the value of A which limits elastic ricochet. Eq. (A.1), as $a\to A$ with $\eta=0$, gives $A=\cos(\theta-\alpha)/\tan\theta$. One may observe that positive α values raise the value of A for a given θ. Thus, for a given A, a minimum θ is obtained only when $\alpha=0$. When $\alpha=0$, the governing relation becomes $A=\cos^2\theta/\sin\theta$. Converting the cosine-squared term to an equivalent sine squared term and solving the resulting quadratic provides the branch I solution, Eq. (14).

A.1.2. Branch III

In branch III, it is the value of β which limits elastic ricochet. Eq. (A.2), as $\beta_{\rm eff}\to\beta$ with $\eta=0$, gives $\beta=\cos\alpha/\sin\theta$. For the $\alpha=0$ limit, this becomes $\beta=1/\sin\theta$ and produces Eq. (17). If α is permitted to be positive and non-zero, the elastic $\theta_{\rm c}$ may be reduced further for a given β. However, the upper limit on α is θ. And so, if α is permitted to take on this upper limit, the governing equation becomes $\beta=1/\tan\theta$, and Eq. (18) follows directly.

A.1.3. Branch II

In branch II, the initial limiting factor is the value of β, and thus the $\alpha=0$ solution, Eq. (20), is identical to that for branch III. However, as α is allowed to increase, the value of A becomes the limiting factor, prior to the point where α increases to a value equal to θ. Thus, for the elastic $\theta_{\rm c}$, both $a\to A$ must be satisfied, as well as $\beta_{\rm eff}\to\beta$. Eq. (A.2), with these limits and $\eta=0$, gives $\cos\alpha=\beta\sin\theta$, which leads to $\sin\alpha=\sqrt{1-\cos^2\alpha}=\sqrt{1-\beta^2\sin^2\theta}$. By expanding $\cos(\theta-\alpha)$ in Eq. (A.1), one obtains

$$A = \cos\alpha\cos^2\theta/\sin\theta + \sin\alpha\cos\theta. \tag{A.6}$$

Substitute the expressions for $\cos\alpha$ and $\sin\alpha$ into Eq. (A.6). Isolate the square root, and square the expression. Reduce the $\beta^2(\sin^2\theta+\cos^2\theta)$ expression to β^2, leaving just an expression for $\cos^2\theta$, which can be solved directly for Eq. (21) (since $\theta=\theta_{\rm c}^{\rm e}$ when $a=A$ and $\beta_{\rm eff}=\beta$). The limiting α value, Eq. (22), is obtained from the earlier expression, $\cos\alpha=\beta\sin\theta$.

A.2. Plastic ricochet ($a=A$)

A.2.1. Solution for a specified β_{eff}

Take Eq. (A.1), solve for $\cos(\theta-\alpha)$, and set aside. In Eq. (A.2), express $(\alpha+\eta)$ as $[(\theta+\eta)-(\theta-\alpha)]$, and expand as a cosine of the sum of angles. Eliminate $\cos(\theta-\alpha)$ from the resulting expression by substituting Eq. (A.1), and solve for $\sin(\theta-\alpha)$. Take these two resulting equations [one for $\cos(\theta-\alpha)$

and the other for $\sin(\theta-\alpha)$], square each of them and add together. The result should be an equation in which α is eliminated:

$$\beta_{\text{eff}}^2 - 1 + A^2\frac{\cos^2\eta}{\cos^2\theta} - 2\beta_{\text{eff}}^2 A\frac{\cos\eta}{\cos\theta}\cos(\theta+\eta) = 0.$$

Expand $\cos(\theta+\eta)$. Clear the denominator. Employ the technique of Eqs. (A.3)–(A.5), so as to obtain $\sin 2\eta$ and hence η. Eq. (23) is analogous to Eq. (A.5), with the terms of Eqs. (24)–(26) corresponding to the coefficients that comprise Eq. (A.5).

Many expressions can be used to obtain α expressions, given β_{eff} and $\eta_{\beta\text{eff}}$, for example solving either Eq. (A.1) or Eq. (A.2) directly for α. However, these expressions solve in terms of an inverse cosine, which cannot, unaided, detect the presence of negative values of α (which are not validly permitted). Instead, start with the expression which was earlier in this section derived for $\sin(\theta-\alpha)$ and take the inverse sine to isolate and obtain Eq. (27).

A.2.2. Solution for which $\alpha=0$

Start with Eq. (A.1). Set $\alpha=0$. Expand $\sin(\theta+\eta)$. Isolate $\cos^2\theta/A$ on one side of the equation. Employ the technique of Eqs. (A.3)–(A.5) to obtain $\sin 2\eta$ as

$$\sin 2\eta = \frac{2}{A}\cos^3\theta - \sin\theta\cos\theta - 2\sin\theta\cos\theta\sqrt{\frac{1}{4}+\frac{\sin\theta}{A}-\frac{\cos^2\theta}{A^2}}. \tag{A.7}$$

A solution to Eq. (A.7) will exist only if the radicand is nonnegative. Consider this radicand inequality to resolve this question and solve for the allowable values of A (only positive A solutions are relevant). The resulting inequality may be expressed in the form of Eq. (28).

Return to Eq. (A.7) to solve for η. In two places, use an Eq. (A.4) substitution. Eq. (29) for η follows.

Eq. (30) follows directly from Eq. (A.2), when α is set to zero.

To prove the assertion that no ricochet solutions exist if Eq. (28) is not satisfied, a similar derivation to Eq. (28) may be obtained, except that, instead of setting α to 0 at the outset, it should be set to a positive constant α_0, for which an alternate solution is sought. The derivable inequality for this condition proves to be

$$2 - A\left(\frac{\cos\theta}{\cos(\theta-\alpha_0)}\right) \leqslant 2\sin\theta \text{ (if } 0<\alpha=\alpha_0\leqslant\theta \text{ solution exists).}$$

But if Eq. (28) is not satisfied, then $2\sin\theta\leqslant(2-A)$ is implied, leading to the requirement that

$$2 - A\left(\frac{\cos\theta}{\cos(\theta-\alpha_0)}\right) \leqslant 2 - A \tag{A.8}$$

be satisfied for an $0<\alpha=\alpha_0\leqslant\theta$ solution to exist simultaneously when there is no $\alpha=0$ solution. Because A is positive, Eq. (A.8) leads to

$$\cos\theta \geqslant \cos(\theta-\alpha_0).$$

However, for $0<\alpha_0\leqslant\theta<\pi/2$, this equation can never be satisfied. One may conclude therefore, if Eq. (28) cannot be satisfied, that no ricochet solution in the range $0<\alpha\leqslant\theta$ can exist.

A.2.3. Solution that maximizes α

Solve Eq. (A.1) for $\cos(\theta-\alpha)$, and call this term k. Expand $\sin(\theta+\eta)$. Employ the technique of Eqs. (A.3)–(A.5) to solve for $\sin 2\eta$:

$$\sin 2\eta = \frac{(2k/A)-\tan\theta-\tan\theta\sqrt{1+(4k\tan\theta/A)-(4k^2/A^2)}}{\tan^2\theta+1}.$$

A solution is possible if the radicand is nonnegative. The maximum allowable α is θ, and so the maximum value for k is unity. When $k=1$, enforcing a nonnegative radicand gives Eq. (31). For the case where the $k=1$

solution exists, substitute $k=1$ and make use of trigonometric identities like $\tan^2\theta+1=\sec^2\theta$ to obtain the η solution of Eq. (32). Eq. (33) is obtained directly from Eq. (A.2) for the case where $\alpha=\theta$.

For cases where the $k=1$ solution is not viable, solve Eq. (A.1) for $\cos(\theta-\alpha)$. Take $\mathrm{d}/\mathrm{d}\eta$ of the equation and set equal to zero, so as to find the value of η for which $\cos(\theta-\alpha)$ is maximized [i.e., where $(\theta-\alpha)$ is minimized]. The solution to this case is $\eta=1/2\sin^{-1}(\cos\theta)=\pi/4-\theta/2$, given as Eq. (34).

Define as k the cosine of this minimized angle, so that $k=\cos(\theta-\alpha)_{\min}$, and substitute into Eq. (A.1); solve for k. Substitute $\eta=\pi/4-\theta/2$ so as to eliminate η, that k may be expressed solely in terms of A and θ. Note that $\cos\eta\,\sin(\theta+\eta)$ may thus be reduced to $1/2\cdot(1+\sin\theta)$, to obtain Eq. (36).

To obtain Eq. (37), first note that $(\alpha+\eta)=-(\theta-\alpha)+(\theta+\eta)$. Using this and the definition of k, upon substitution into Eq. (A.2), gives

$$\beta=\sqrt{1-k^2}+\frac{k}{\tan(\theta+\eta)}. \tag{A.9}$$

Conversely, the definition of k into Eq. (A.1) gives, with some regrouping,

$$\frac{k}{\tan(\theta+\eta)}=\frac{A}{\cos\theta}\cos\eta\,\cos(\theta+\eta) \tag{A.10}$$

Substituting Eq. (A.10) into Eq. (A.9), to eliminate $k/\tan(\theta+\eta)$, gives

$$\beta=\sqrt{1-k^2}+\frac{A}{\cos\theta}\cos\eta\,\cos(\theta+\eta). \tag{A.11}$$

Knowing $\eta=\pi/4-\theta/2$ allows one to determine that $\cos\eta\,\cos(\theta+\eta)=(\cos\theta)/2$. This result reduces Eq. (A.11) to Eq. (37).

A.2.4. Solution for which $\alpha=\eta$

Start with Eq. (A.1), and isolate $\cos(\theta-\alpha)$. Expand sine and cosine terms for the angle sums. Multiply the equation by $\sec^2\eta$, so that all η terms appear as tangents and secants. Square the equation, substitute $(1+\tan^2\eta)$ for $\sec^2\eta$, and expand the terms so that all η terms appear as powers of $\tan\eta$ terms. Move all the terms to one side of the equation, and group by powers of $\tan\eta$. Divide the equation by $\sin^2\theta$, which is the multiplier on the $\tan^4\eta$ term, in order to obtain a fourth order equation with $\tan^4\eta$ as the leading term. Finally, factor out a $\cos\theta$ from the denominator of the $\tan\eta$ multiplier, and use a double angle formula in θ, to obtain Eq. (38).

To obtain the simple, large-A limit to η, Eq. (39), start with Eq. (A.1) and approximate all cosine terms as having a value of 1. Solve for η.

To obtain the accurate approximation, Eq. (40), start with Eq. (A.1) and substitute η^* for α. Put all terms involving η on one side of the equation. Expand the $\sin(\theta+\eta)$ term. Use the technique of Eqs. (A.3)–(A.5) to solve for $\sin 2\eta$, where $r=1$, $p=1/\tan\theta$, and $q=1-E$, using the term grouping for E in Eq. (41). A straightforward ($\sec^2\theta=1+\tan^2\theta$) trigonometric substitution is needed in the denominator in order to obtain Eq. (40).

Eq. (42) is obtained from Eq. (A.2), by setting α to η.

A.2.5. Solution for which $\eta=0$

From Eq. (A.1), substituting $\eta=0$, one may directly obtain the manuscript's expression for Eq. (44), by noting that $\cos(\theta-\alpha)=A\tan\theta$. To obtain the expression for Eq. (43), combine Eqs. (A.1) and (A.2) (with $\eta=0$) to obtain

$$\beta=\frac{A\cos\alpha}{\cos(\theta-\alpha)\cos\theta}. \tag{A.12}$$

By evaluating $\cos\alpha$ as $\cos[\theta-(\theta-\alpha)]$, expanding it, and utilizing the fact that $\cos(\theta-\alpha)=\mathrm{A}\tan\theta$, the expression for Eq. (43) may be directly obtained from Eq. (A.12).

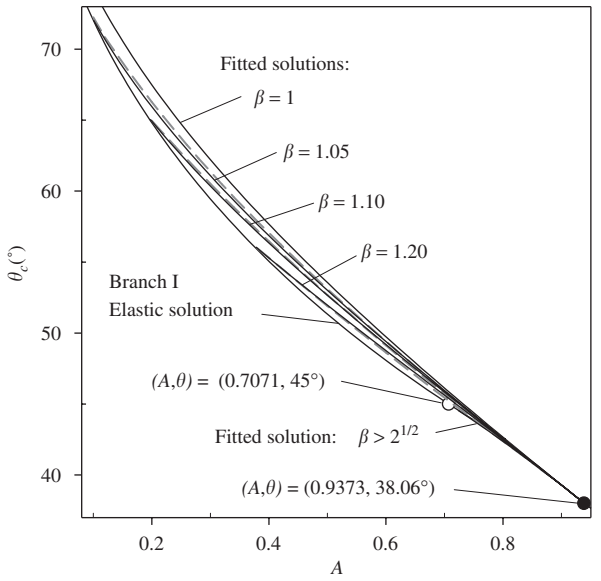

Fig. B1. Empirical fit for critical ricochet obliquity, with β as a parameter, applicable for $\theta_c \geqslant 38.33^\circ$. Fitted curves are depicted as solid lines. Actual general-model behavior is depicted with dashed lines.

Appendix B. Mode IV-x discussion

Mode IV-x ricochet, as depicted in Fig. 5e, plays a role in the critical obliquity only within the small triangular (A,θ_c) region delimited by the vertices $(1/\sqrt{2}, 45^\circ)$, $(0.9373, 38.06^\circ)$, and $(0.8047, 42.497^\circ)$. To show a vertex of the Mode IV-x region at $(1/\sqrt{2}, 45^\circ)$, insert this (A,θ_c) point into Eq. (38) to obtain the four roots of $\tan \eta_{\alpha=\eta}$ as $(0,0,-1,-1)$. The double roots at $\eta = 0$ indicate a terminus of the Mode IV-x region. Similarly, when the (A,θ_c) values associated with the vertex $(0.9373, 38.06^\circ)$ are entered into Eq. (38), a double root at $\eta = 17.31^\circ$ ($\beta_{\text{eff}} = 1$) is produced, indicating the other Mode IV-x terminus for large-β ricochet. At the third vertex of the region, $(0.8047, 42.497^\circ)$, there is one root at $\alpha = \eta = 0$ and one at $\eta = 15.83^\circ$ ($\beta_{\text{eff}} = 1$).

If one were to attempt an empirical characterization of the Mode IV-x solutions, it proves convenient to note (from Fig. 5e for example) that the $\alpha = \eta$ solution associated with the Mode IV-x limit condition (where A is lowered to the point where the α and η curves are tangent at a single point) is diminished in magnitude with respect to the $\alpha = \eta$ solution associated with the $\beta = 1$ condition. We therefore employ a form for the finitely diminished α_c that mirrors the form of the perturbation analysis used in Eqs. (55)–(56), which lends itself to ready characterization of the Mode IV-x solution curve for large β, as

$$\alpha_c = \eta_c = 30^\circ - \theta_c/3 - \Delta\alpha \text{ (when } 38.06^\circ \leqslant \theta_c \leqslant \theta_{\alpha=0}) \tag{B.1}$$

leading to

$$A = \frac{\cos\big((4\theta_c/3) - 30^\circ + \Delta\alpha\big)\cos\,\theta_c}{\sin\big((2\theta_c/3) + 30^\circ - \Delta\alpha\big)\cos\big((\theta_c/3) - 30^\circ + \Delta\alpha\big)} \text{ (when } 38.06^\circ \leqslant \theta_c \leqslant \theta_{\alpha=0}), \tag{B.2}$$

where $\theta_{\alpha=0}$ is the angle where this fitted form for Mode IV-x solutions merges with the elastic solution, in this case at $\theta_{\alpha=0} = 45^\circ$. The near linearity of the diminishment of α that is noted in Fig. 5e suggests that the $\Delta\alpha$ function may be empirically characterized with the linear approximation

$$\Delta\alpha \approx 2.161(\theta_c - 38.06^\circ) \text{ (when } 38.06^\circ \leqslant \theta_c \leqslant 45^\circ). \tag{B.3}$$

Eq. (B.3) guarantees that α_c take on the proper value at $\theta_c = 38.06^\circ$, associated with the $\beta = 1$ solution, and that it takes on a value of $\alpha_c = 0$ at $\theta_c = 45^\circ$.

While the result was not shown in Fig. 11, it lays virtually atop the Mode IV-x solution curve for large β. In this case, large β are defined as being in excess of $\sqrt{2}$, since the upper limit of this fit, at $\theta_c = 45^\circ$, $A = 1/\sqrt{2}$, which blends into the $\alpha = 0$ elastic solution, has a value of β_{eff} equal to $\sqrt{2}$ at that point.

In fact, one may use this same technique to empirically approximate, not only the Mode IV-x solutions, but all the limiting ($\alpha_c = \eta_c$) plastic solutions that lie between the $\beta = 1$ solution and the branch I elastic solution ($\beta > \sqrt{2}$), for which no analytical function is otherwise offered. One adopts the form of Eqs. (B.1)–(B.2), utilizing the $\Delta\alpha$ diminishment term, except that $\theta_{\alpha=0}$ is no longer fixed at a value of 45°. Rather, the upper limit of the fit, at $\theta_{\alpha=0}$, defining the point where the fit merges with the elastic solution, varies with β according to elastic ricochet relation,

$$\theta_{\alpha=0} = \sin^{-1}(1/\beta_{\text{eff}}). \tag{B.4}$$

The $\Delta\alpha$ function must be empirically characterized to force α_c to a value of zero at the point where $\theta_c = \theta_{\alpha=0}$. Linearly fit to this constraint, the value of $\Delta\alpha$ is generalized to

$$\Delta\alpha = \frac{\theta_c - 38.06^\circ}{\theta_{\alpha=0} - 38.06^\circ}(30^\circ - \theta_{\alpha=0}/3).$$

By setting $\beta_{\text{eff}} = \min[\beta, \sqrt{2}]$, the Mode IV-x fit is recovered for $\beta > \sqrt{2}$. At the lower limit of $\beta = 1$, Eq. (B.4) indicates that $\theta_{\alpha=0} = 90^\circ$; and so $\Delta\alpha \equiv 0$, which allows the exact $\beta = 1$ solution to be recovered, as well.

Fig. B1 shows the quality of this fit for predicting the critical ricochet obliquity for intermediate values of β. In the figure, the fitted predictions are drawn with solid lines, while the model's true behavior, acquired through a systematic application of the general solution, is shown with dashed lines. One may observe that this empirical fit for the critical ricochet angle does an excellent job of matching the general model results, over the complete range of β. Because this fit is empirical, however, it was not incorporated into the contents of Table 2.

References

[1] Segletes SB. A rod ricochet model. US Army Research Laboratory technical report ARL-TR-3257, Aberdeen Proving Ground, Maryland, August 2004.
[2] Segletes SB. A model for rod ricochet. Int J Impact Eng 2006;32:1403–39.
[3] Senf HH, Rothenhaeusler, Scharpf , Poth A, Pfang W. Experimental and numerical investigation of the ricocheting of projectiles from metallic surfaces. In: Proceedings of the sixth International Symposium on Ballistics, Orlando, FL 1981. p. 510–21.
[4] Beyer WH, editor. CRC standard mathematical tables, 26th. Boca Raton, FL, CRC Press; 1986. p.12.
[5] Tate A. A simple estimate of the minimum target obliquity required for the ricochet of a high speed long rod projectile. J Phys D: Appl Phys 1979;12:1825–9.
[6] Rosenberg Z, Yeshurun Y, Mayseless M. On the ricochet of long rod projectiles. In: Proceedings of the 11th International Symosium on Ballistics, Brussels, Belgium, 1989.p. TB-28/1–TB-28/6.

NO. OF COPIES	ORGANIZATION
1 (PDF ONLY)	DEFENSE TECHNICAL INFORMATION CTR DTIC OCA 8725 JOHN J KINGMAN RD STE 0944 FORT BELVOIR VA 22060-6218
1	US ARMY RSRCH DEV & ENGRG CMD SYSTEMS OF SYSTEMS INTEGRATION AMSRD SS T 6000 6TH ST STE 100 FORT BELVOIR VA 22060-5608
1	DIRECTOR US ARMY RESEARCH LAB IMNE ALC IMS 2800 POWDER MILL RD ADELPHI MD 20783-1197
3	DIRECTOR US ARMY RESEARCH LAB AMSRD ARL CI OK TL 2800 POWDER MILL RD ADELPHI MD 20783-1197

ABERDEEN PROVING GROUND

1	DIR USARL AMSRD ARL CI OK TP (BLDG 4600)

NO. OF COPIES ORGANIZATION

1 COMMANDER
US ARMY ARDEC
AMSTA AAR AEM T
M D NICOLICH
BLDG 65S
PICATINNY ARSENAL NJ 07806-5000

1 COMMANDER
US ARMY ARDEC
AMSRD AAR AEW M(D)
M MINISI
BLDG 65N
PICATINNY ARSENAL NJ 07806-5000

3 COMMANDER
US ARMY AVN & MIS CMND
AMSAM RD PS WF
D LOVELACE
M SCHEXNAYDER
G SNYDER
REDSTONE ARSENAL AL 35898

1 COMMANDER
US ARMY AVN & MIS CMND
AMSAM RD SS AA
J BILLINGSLEY
REDSTONE ARSENAL AL 35898

3 COMMANDER
US ARMY RSRCH OFC
K IYER
J BAILEY
S F DAVIS
PO BOX 12211
RSRCH TRIANGLE PARK NC
27709-2211

1 NAVAL AIR WARFARE CTR
S A FINNEGAN
BOX 1018
RIDGECREST CA 93556

3 COMMANDER
NAVAL WEAPONS CTR
T T YEE CODE 3263
D THOMPSON CODE 3268
W J MCCARTER CODE 6214
CHINA LAKE CA 93555

1 USAF PHILLIPS LAB
VTSI
R ROYBAL
KIRTLAND AFB NM 87117-7345

NO. OF COPIES ORGANIZATION

1 AFIT ENC
D A FULK
WRIGHT PATTERSON AFB OH 45433

5 COMMANDER
NAVAL SURFACE WARFARE CTR
DAHLGREN DIV
D L DICKINSON CODE G24
C R ELLINGTON
W HOLT CODE G22
R MCKEOWN
W J STROTHER
17320 DAHLGREN RD
DAHLGREN VA 22448

1 AIR FORCE ARMAMENT LAB
AFATL DLJR
D LAMBERT
EGLIN AFB FL 32542-6810

1 FEDERAL BUREAU OF INVESTIGATION
FBI LAB EXPLOSIVES UNIT
M G LEONE
935 PENNSYLVANIA AVE NW
WASHINGTON DC 20535

7 LOS ALAMOS NATL LAB
L HULL MS A133
J WALTER MS C305
C WINGATE MS D413
C RAGAN MS D449
E J CHAPYAK MS F664
J BOLSTAD MS G787
P HOWE MS P915
PO BOX 1663
LOS ALAMOS NM 87545

4 DIRECTOR
LLNL
MS L35
ROBERT E TIPTON L35
DENNIS BAUM L35
MICHAEL MURPHY L35
TOM MCABEE L35
PO BOX 808
LIVERMORE CA 94550

NO. OF COPIES ORGANIZATION

1 DIRECTOR
LLNL
RUSSELL ROSINKY L122
PO BOX 808
LIVERMORE CA 94550

21 SANDIA NATIONAL LABS
MAIL SVC MS0100
A ROBINSON MS0378
W TEDESCHI MS1219
B LEVIN MS0706
T TRUCANO MS0370
P TAYLOR MS0378
D B LONGCOPE MS0372
M KIPP MS0378
D CRAWFORD MS0836
L CHHABILDAS MS1181
E S HERTEL JR MS0836
L N KMETYK MS0847
R LAFARGE MS0674
R TACHAU MS1007
M FURNISH MS1168
W REINHART MS1181
D P KELLY MS1185
C HALL MS1209
J COREY MS1217
C HILLS MS1411
R O NELLUMS MS0325
T VOGLER
PO BOX 5800
ALBUQUERQUE NM 87185-0100

2 DIRECTOR
LLNL
GLENN POMYKAL L178
MICHAEL GERASSIMENKO L178
PO BOX 808
LIVERMORE CA 94550

1 DIRECTOR
LLNL
WILLIAM C TAO L282
PO BOX 808
LIVERMORE CA 94550

1 DIRECTOR
LLNL
JACK E REAUGH L290
PO BOX 808
LIVERMORE CA 94550

NO. OF COPIES ORGANIZATION

1 DIRECTOR
LLNL
ROBERT M KUKLO L874
PO BOX 808
LIVERMORE CA 94550

3 NASA
JOHNSON SPACE CTR
E CHRISTIANSEN
J L CREWS
F HORZ
MAIL CODE SN3
2101 NASA RD 1
HOUSTON TX 77058

2 CALTECH
J SHEPHERD MS 105 50
A P INGERSOLL MS 170 25
1201 E CALIFORNIA BLVD
PASADENA CA 91125

1 CALTECH
G ORTON MS 169 237
4800 OAK GROVE DR
PASADENA CA 91007

5 JOHNS HOPKINS UNIV
APPLIED PHYSICS LAB
T R BETZER
A R EATON
R H KEITH
D K PACE
R L WEST
JOHNS HOPKINS RD
LAUREL MD 20723

1 LOUISIANA STATE UNIV
R W COURTER
948 WYLIE DR
BATON ROUGE LA 70808

4 SOUTHWEST RSRCH INST
C ANDERSON
S A MULLIN
J RIEGEL
J WALKER
PO DRAWER 28510
SAN ANTONIO TX 78228-0510

1 SUNY STONEYBROOK
DEPT APPL MATH & STAT
J GLIMM
STONEYBROOK NY 11794

NO. OF COPIES ORGANIZATION

1 TEXAS A&M UNIV
PHYSICS DEPT
D BRUTON
COLLEGE STATION TX 77843-4242

2 UC SAN DIEGO
DEPT APPL MECH & ENGRG
SVCS R011
S NEMAT-NASSER
M MEYERS
LA JOLLA CA 92093-0411

1 UNIV OF ALABAMA BIRMINGHAM
HOEN 101
D LITTLEFIELD
1530 3RD AVE
BIRMINGHAM AL 35294-4440

2 UNIV OF ALABAMA HUNTSVILLE
AEROPHYSICS RSRCH CTR
G HOUGH
D J LIQUORNIK
PO BOX 999
HUNTSVILLE AL 35899

2 UNIV OF DAYTON RSRCH INST
N BRAR
A PIEKUTOWSKI
300 COLLEGE PARK
DAYTON OH 45469-0182

3 UNIV OF DELAWARE
DEPT OF MECH ENGRG
J GILLESPIE
J VINSON
D WILKINS
NEWARK DE 19716

1 UNIV OF MISSOURI ROLLA
CA&E ENGRG
W P SCHONBERG
1870 MINER CIR
ROLLA MO 65409

1 UNIV OF TEXAS
DEPT OF MECHL ENGRG
E P FAHRENTHOLD
AUSTIN TX 78712

NO. OF COPIES ORGANIZATION

1 UNIV OF UTAH
DEPT OF MECH ENGRG
R BRANNON
50 S CENTRAL CAMPUS DR
RM 2110
SALT LAKE CITY UT 84112-9208

1 VIRGINIA POLYTECHNIC INST
COLLEGE OF ENGRG
DEPT ENGRG SCI & MECHS
R C BATRA
BLACKSBURG VA 24061-0219

2 AEROJET ORDNANCE
P WOLF
G PADGETT
1100 BULLOCH BLVD
SOCORRO NM 87801

2 APPLIED RSRCH ASSOC INC
D GRADY
F MAESTAS
STE A220
4300 SAN MATEO BLVD NE
ALBUQUERQUE NM 87110

1 APPLIED RSRCH LAB
J A COOK
10000 BURNETT RD
AUSTIN TX 78758

1 BAE SYS ANALYTICAL
SOLUTIONS INC
M B RICHARDSON
308 VOYAGER WAY
HUNTSVILLE AL 35806

1 COMPUTATIONAL MECHS
CONSULTANTS
J A ZUKAS
PO BOX 11314
BALTIMORE MD 21239-0314

1 CYPRESS INTERNATIONAL
A CAPONECCHI
1201 E ABINGDON DR
ALEXANDRIA VA 22314

2 DE TECHNOLOGIES INC
R CICCARELLI
W FLIS
3620 HORIZON DR
KING OF PRUSSIA PA 19406

NO. OF COPIES ORGANIZATION

3 DOW CHEMICAL INC
ORDNANCE SYS
C HANEY
A HART
B RAFANIELLO
800 BLDG
MIDLAND MI 48667

3 DYNASEN
J CHAREST
M CHAREST
M LILLY
20 ARNOLD PL
GOLETA CA 93117

1 R J EICHELBERGER
409 W CATHERINE ST
BEL AIR MD 21014-3613

1 ELORET INST
NASA AMES RSRCH CTR
D W BOGDANOFF MS 230 2
MOFFETT FIELD CA 94035

1 EXPLOSIVE TECHLGY
M L KNAEBEL
PO BOX KK
FAIRFIELD CA 94533

1 GB TECH LOCKHEED
J LAUGHMAN
2200 SPACE PARK STE 400
HOUSTON TX 77258

2 GB TECH LOCKHEED
L BORREGO C23C
J FALCON JR C23C
2400 NASA RD 1
HOUSTON TX 77058

6 GDLS
38500 MOUND RD
W BURKE MZ436 21 24
G CAMPBELL MZ436 30 44
D DEBUSSCHER MZ436 20 29
J ERIDON MZ436 21 24
W HERMAN MZ 435 01 24
S PENTESCU MZ436 21 24
STERLING HTS MI 48310-3200

NO. OF COPIES ORGANIZATION

3 GD OTS
D A MATUSKA
M GUNGER
J OSBORN
4565 COMMERCIAL DR #A
NICEVILLE FL 32578

2 GD OTS
D BOEKA
N OUYE
2950 MERCED ST
STE 131
SAN LEANDRO CA 94577

1 GENERAL RSRCH CORP
T MENNA
PO BOX 6770
SANTA BARBARA CA 93160-6770

4 INST FOR ADVANCED TECHLGY
S J BLESS
J CAZAMIAS
J DAVIS
H D FAIR
3925 W BRAKER LN
AUSTIN TX 78759-5316

1 INTERNATIONAL RSRCH ASSOC
D L ORPHAL
4450 BLACK AVE
PLEASANTON CA 94566

1 R JAMESON
624 ROWE DR
ABERDEEN MD 21001

1 KAMAN SCIENCES CORP
D L JONES
2560 HUNTINGTON AVE STE 200
ALEXANDRIA VA 22303

1 LOCKHEED MARTIN ELEC & MIS
G W BROOKS
5600 SAND LAKE RD MP 544
ORLANDO FL 32819-8907

1 LOCKHEED MARTIN
MIS & SPACE
W R EBERLE
PO BOX 070017
HUNTSVILLE AL 35807

NO. OF COPIES ORGANIZATION

3 LOCKHEED MARTIN
MIS & SPACE
M A LEVIN ORG 81 06 BLDG 598
M R MCHENRY
T A NGO ORG 81 10 BLDG 157
111 LOCKHEED WAY
SUNNYVALE CA 94088

4 LOCKHEED MIS & SPACE CO
J R ANDERSON
W C KNUDSON
S KUSUMI 0 81 11 BLDG 157
J PHILLIPS 0 54 50
PO BOX 3504
SUNNYVALE CA 94088

1 LOCKHEED MIS & SPACE CO
R HOFFMAN
SANTA CRUZ FACILITY
EMPIRE GRADE RD
SANTA CRUZ CA 95060

1 MCDONNELL DOUGLAS
ASTRNTCS CO
B L COOPER
5301 BOLSA AVE
HUNTINGTON BEACH CA 92647

2 NETWORK COMPUTING SVC INC
T HOLMQUIST
G JOHNSON
1200 WASHINGTON AVE S
MINNEAPOLIS MN 55415

1 PHYSICAL SCIENCES INC
P NEBOLSINE
20 NEW ENGLAND BUS CTR
ANDOVER MA 01810

1 RAYTHEON ELECTRONIC SYS
R LLOYD
50 APPLE HILL DR
TEWKSBURY MA 01876

1 ROCKWELL INTERNATIONAL
ROCKETDYNE DIV
H LEIFER
16557 PARK LN CIR
LOS ANGELES CA 90049

1 SAIC
M W MCKAY
10260 CAMPUS POINT DR
SAN DIEGO CA 92121

NO. OF COPIES ORGANIZATION

1 SHOCK TRANSIENTS INC
D DAVISON
BOX 5357
HOPKINS MN 55343

2 SOUTHERN RSRCH INST
L A DECKARD
D P SEGERS
PO BOX 55305
BIRMINGHAM AL 35255-5305

1 ZERNOW TECHNICAL SVCS INC
L ZERNOW
425 W BONITA AVE STE 208
SAN DIMAS CA 91773

ABERDEEN PROVING GROUND

67 DIR USARL
AMSRD ARL SL
P TANENBAUM
AMSRD ARL SL BB
R DIBELKA
E HUNT
J ROBERTSON
AMSRD ARL SL BD
R GROTE
L MOSS
J POLESNE
AMSRD ARL SL BM
D FARENWALD
D BELY
G BRADLEY
M OMALLEY
R SAUCIER
A DIETRICH
AMSRD ARL SL BS
M BURDESHAW
AMSRD ARL WM
T W WRIGHT
AMSRD ARL WM BD
A ZIELINSKI
AMSRD ARL WM MB
W DEROSSET
AMSRD ARL WM MD
E CHIN
G GAZONAS
J LASALVIA
AMSRD ARL WM TA
S SCHOENFELD
M BURKINS
N GNIAZDOWSKI
W A GOOCH

NO. OF
COPIES ORGANIZATION

C HOPPEL
E HORWATH
D KLEPONIS
B LEAVY
M LOVE
J RUNYEON
AMSRD ARL WM TB
R BITTING
J STARKENBERG
AMSRD ARL WM TC
R COATES
R ANDERSON
J BARB
N BRUCHEY
T EHLERS
T FARRAND
M FERMEN-COKER
E KENNEDY
K KIMSEY
L MAGNESS
B PETERSON
D SCHEFFLER
S SCHRAML
A SIEGFRIED
B SORENSEN
R SUMMERS
W WALTERS
C WILLIAMS
G RANDERS-PEHRSON
AMSRD ARL WM TD
T W BJERKE
S BILYK
D CASEM
J CLAYTON
D DANDEKAR
M GRINFELD
Y I HUANG
K IYER
B LOVE
M RAFTENBERG
E RAPACKI
M SCHEIDLER
S SEGLETES
T WEERASOORIYA
H W MEYER
AMSRD ARL WM TE
J POWELL

NO. OF COPIES ORGANIZATION

2 AERONAUTICAL & MARITIME
RSRCH LAB
S CIMPOERU
D PAUL
PO BOX 4331
MELBOURNE VIC 3001
AUSTRALIA

1 DSTO AMRL
WEAPONS SYS DIV
N BURMAN (RLLWS)
SALISBURY
SOUTH AUSTRALIA 5108
AUSTRALIA

1 ROYAL MILITARY ACADEMY
G DYCKMANS
RENAISSANCELAAN 30
1000 BRUSSELS
BELGIUM

1 CANADIAN ARSENALS LTD
P PELLETIER
5 MONTEE DES ARSENAUX
VILLIE DE GRADEUR PQ J5Z2
CANADA

1 DEFENCE RSRCH ESTAB SUFFIELD
D MACKAY
RALSTON ALBERTA TOJ 2NO
RALSTON
CANADA

1 DEFENCE RSRCH ESTAB SUFFIELD
C WEICKERT
BOX 4000 MEDICINE HAT
ALBERTA TIA 8K6
CANADA

1 DEFENCE RSRCH ESTAB
VALCARTIER
ARMAMENTS DIV
R DELAGRAVE
2459 PIE X1 BLVD N
PO BOX 8800
CORCELETTE QUEBEC GOA 1R0
CANADA

1 CEA/CESTA
A GEILLE
BOX 2 LE BARP 33114
FRANCE

NO. OF COPIES ORGANIZATION

5 CENTRE D'ETUDES DE GRAMAT
C LOUPIAS
P OUTREBON
J CAGNOUX
C GALLIC
J TRANCHET
GRAMAT 46500
FRANCE

1 DAT ETBS CETAM
C ALTMAYER
ROUTE DE GUERRY BOURGES
18015
FRANCE

1 FRENCH GERMAN RSRCH INST
P-Y CHANTERET
CEDEX 12 RUE DE L'INDUSTRIE
BP 301
F68301 SAINT-LOUIS
FRANCE

5 FRENCH GERMAN RSRCH INST
H-J ERNST
F JAMET
P LEHMANN
K HOOG
H F LEHR
CEDEX 5 5 RUE DU GENERAL
CASSAGNOU
SAINT LOUIS 68301
FRANCE

1 CONDAT
J KIERMEIR
MAXIMILIANSTR 28
8069 SCHEYERN FERNHAG
GERMANY

1 TDW
M HELD
POSTFACH 13 40
D 86523 SCHROBENHAUSEN
GERMANY

1 DIEHL GBMH AND CO
M SCHILDKNECHT
FISCHBACHSTRASSE 16
D 90552 ROETBENBACH AD PEGNITZ
GERMANY

NO. OF COPIES ORGANIZATION

4 ERNST MACH INSTITUT
V HOHLER
E SCHMOLINSKE
E SCHNEIDER
K THOMA
ECKERSTRASSE 4
D-7800 FREIBURG I BR 791 4
GERMANY

3 FRAUNHOFER INSTITUT FUER KURZZEITDYNAMIK
ERNST MACH INSTITUT
H ROTHENHAEUSLER
H SENF
E STRASSBURGER
KLINGELBERG 1
D79588 EFRINGEN-KIRCHEN
GERMANY

3 FRENCH GERMAN RSRCH INST
G WEIHRAUCH
R HUNKLER
E WOLLMANN
POSTFACH 1260
WEIL AM RHEIN D-79574
GERMANY

2 IABG
M BORRMANN
H G DORSCH
EINSTEINSTRASSE 20
D 8012 OTTOBRUN B MUENCHEN
GERMANY

1 INGENIEURBUERO DEISENROTH
AUF DE HARDT 33 35
D5204 LOHMAR 1
GERMANY

1 NORDMETALL GMBH
L W MEYER
EIBENBERG
EINSIEDLER STR 18 H
D-09235 BURKHARDTSDORF
GERMANY

2 TU CHEMNITZ
L W MEYER (X2)
FAKULTAET FUER MASCHINENBAU
LEHRSTUHL WERKSTOFFE DES MASCHINENBAUS
D-09107 CHEMNITZ
GERMANY

NO. OF COPIES ORGANIZATION

5 RAFAEL BALLISTICS CTR
E DEKEL
Y PARTOM
G ROSENBERG
Z ROSENBERG
Y YESHURUN
PO BOX 2250
HAIFA 31021
ISRAEL

1 TECHNION INST OF TECH
FACULTY OF MECH ENGNG
S BODNER
TECHNION CITY
HAIFA 32000
ISRAEL

1 ESTEC CS
D CASWELL
BOX 200 NOORDWIJK
2200 AG
NETHERLANDS

2 PRINS MAURITS LAB
H J REITSMA
E VAN RIET
TNO BOX 45
RIJSWIJK 2280AA
NETHERLANDS

1 TNO DEFENSE, SECURITY AND SAFETY
R ISSELSTEIN
PO BOX 96864
THE HAGUE 2509JG
NETHERLANDS

1 ROYAL NETHERLANDS ARMY
J HOENEVELD
V D BURCHLAAN 31
PO BOX 90822
2509 LS THE HAGUE
NETHERLANDS

1 INST OF CHEMICAL PHYSICS
A YU DOLGOBORODOV
KOSYGIN ST 4 V 334
MOSCOW
RUSSIA

NO. OF COPIES ORGANIZATION

3 INST OF CHEMICAL PHYSICS
RUSSIAN ACADEMY OF SCIENCES
G I KANEL
S V RAZORENOV
A V UTKIN
142432 CHERNOGOLOVKA
MOSCOW REGION
RUSSIA

1 INST OF EARTHS CRUST
P I DOROGOKUPETS
664033 IRKUTSK
RUSSIA

3 INST OF MECHL ENGRG PROBLEMS
V BULATOV
D INDEITSEV
Y MESCHERYAKOV
BOLSHOY, 61, V.O.
ST PETERSBURG 199178
RUSSIA

1 INST OF MINEROLOGY & PETROGRAPHY
V A DREBUSHCHAK
UNIVERSITETSKI PROSPEKT, 3
630090 NOVOSIBIRSK
RUSSIA

2 IOFFE PHYSICO TECHNICAL INST
DENSE PLASMA DYNAMICS LAB
E M DROBYSHEVSKI
A KOZHUSHKO
ST PETERSBURG 194021
RUSSIA

1 IPE RAS
A A BOGOMAZ
DVORTSOVAIA NAB 18
ST PETERSBURG
RUSSIA

2 LAVRENTYEV INST HYDRODYNAMICS
L A MERZHIEVSKY
V V SILVESTROV
630090 NOVOSIBIRSK
RUSSIA

1 MOSCOW INST OF PHYSICS & TECH
S V UTYUZHNIKOV
DEPT OF COMPTNL MATH
DOLGOPRUDNY 1471700
RUSSIA

NO. OF COPIES ORGANIZATION

1 RSRCH INST OF MECHS
NIZHNIY NOVGOROD STATE UNIV
A SADYRIN
P R GAYARINA 23 KORP 6
NIZHNIY NOVGOROD 603600
RUSSIA

1 SAMARA STATE AEROSPACE UNIV
L G LUKASHEV
SAMARA
RUSSIA

1 TOMSK STATE UNIV
A G GERASIMOV
5-TH ARMY ST 29-61
TOMSK 634024
RUSSIA

1 DYNAMEC RSRCH AB
A PERSSON
PO BOX 201
SE-15123 SÖDERTÄLJE
SWEDEN

7 FOI
SWEDISH DEFENCE RSRCH AGENCY
GRINDSJON RSRCH CENTRE
L GUNNAR OLSSON
B JANZON
G WIJK
R HOLMLIN
C LAMNEVIK
L FAST
M JACOB
SE-14725 TUMBA
SWEDEN

2 SWEDISH DEFENCE RSRCH ESTAB
DIV OF MATERIALS
S J SAVAGE
J ERIKSON
S-17290 STOCKHOLM
SWEDEN

2 K&W THUN
W LANZ
W ODERMATT
ALLMENDSSTRASSE 86
CH-3602 THUN
SWITZERLAND

NO. OF
COPIES ORGANIZATION

5 DERA
I CULLIS
J P CURTIS Q13
A HART Q13
K COWAN Q13
M FIRTH R31
FORT HALSTEAD
SEVENOAKS KENT TN14 7BP
UNITED KINGDOM

1 UK MINISTRY OF DEFENCE
G J CAMBRAY
CBDE PORTON DOWN SALISBURY
WITTSHIRE SPR 0JQ
UNITED KINGDOM

7 INST FOR PROBLEMS IN
MATERIALS SCIENCE
S FIRSTOV
B GALANOV
O GRIGORIEV
V KARTUZOV
V KOVTUN
Y MILMAN
V TREFILOV
3 KRHYZHANOVSKY STR
252142 KIEV-142
UKRAINE

1 INST FOR PROBLEMS OF STRENGTH
G STEPANOV
TIMIRYAZEVSKAYU STR 2
252014 KIEV
UKRAINE